UNCERTAINTY QUANTIFICATION AND RELIABILITY ANALYSIS
OF EXISTING CONCRETE BRIDGES
USING REAL AND UPDATED TRAFFIC LOADS

FERNANDO MERLIM DE OLIVEIRA

DISSERTAÇÃO DE MESTRADO EM ESTRUTURAS E CONSTRUÇÃO CIVIL
DEPARTAMENTO DE ENGENHARIA CIVIL E AMBIENTAL

FACULDADE DE TECNOLOGIA

UNIVERSIDADE DE BRASÍLIA

UNIVERSIDADE DE BRASÍLIA
FACULDADE DE TECNOLOGIA
DEPARTAMENTO DE ENGENHARIA CIVIL E AMBIENTAL

UNCERTAINTY QUANTIFICATION AND RELIABILITY ANALYSIS
OF EXISTING CONCRETE BRIDGES
USING REAL AND UPDATED TRAFFIC LOADS

FERNANDO MERLIM DE OLIVEIRA

ORIENTADOR: FRANCISCO EVANGELISTA JÚNIOR
DISSERTAÇÃO DE MESTRADO EM ESTRUTURAS E CONSTRUÇÃO CIVIL

PUBLICAÇÃO: DM 04A/23
BRASÍLIA/DF: FEVEREIRO – 2023

DEPARTAMENTO DE ENGENHARIA CIVIL E AMBIENTAL

**UNCERTAINTY QUANTIFICATION AND RELIABILITY ANALYSIS
OF EXISTING CONCRETE BRIDGES
USING REAL AND UPDATED TRAFFIC LOADS**

FERNANDO MERLIM DE OLIVEIRA

DISSERTAÇÃO DE MESTRADO SUBMETIDA AO DEPARTAMENTO DE ENGENHARIA CIVIL E AMBIENTAL DA FACULDADE DE TECNOLOGIA DA UNIVERSIDADE DE BRASÍLIA COMO PARTE DOS REQUISITOS NECESSÁRIOS PARA A OBTENÇÃO DO GRAU DE MESTRE EM ESTRUTURAS E CONSTRUÇÃO CIVIL.

APROVADA POR:

_____
Prof. Francisco Evangelista Junior, PhD. (ENC/UnB)
(Orientador)

_____
Prof. Ramon Saleno Yure Rubim Costa Silva, DSc. (ENC/UnB)

(Examinador Interno)

_____
Prof. Gelson de Sousa Alves, DSc. (UFPI)
(Examinador Externo)

Brasília/DF, 17 de fevereiro de 2023

FICHA CATALOGRÁFICA

REFERÊNCIA BIBLIOGRÁFICA

OLIVEIRA, F. M (2023). Uncertainty quantification and reliability analysis of existing concrete bridges using real and updated traffic loads. Dissertação de Mestrado em Estruturas e Construção Civil, Publicação DM 04A/23, Departamento de Engenharia Civil e Ambiental, Universidade de Brasília, Brasília, DF, 71 p.

CESSÃO DE DIREITOS

AUTOR: Fernando Merlim de Oliveira

TÍTULO: UNCERTAINTY QUANTIFICATION AND RELIABILITY ANALYSIS OF EXISTING CONCRETE BRIDGES USING REAL AND UPDATED TRAFFIC LOADS

GRAU: Mestre   ANO: 2023

_____

Fernando Merlim de Oliveira
SQNW 311 Bloco C Ap. 315B
CEP: 70687-315 Brasília – DF – Brasil
e-mail: merlim.fmo@gmail.com

ACKNOWLEDGMENTS

To my wife Gláucia, who always supported me during the research phase, giving me the strength to continue and always being my reference.

To my parents, who have always encouraged me since I was a child to pursue the path of education.

To my sister, who believed in the development of this research.

To my friends, who were always by my side following and encouraging this academic journey.

To my advisor Francisco Evangelista Junior, who made several suggestions that enhanced this work.

To the board members, professors Ramon Saleno and Gelson de Sousa, who made recommendations that made the work more complete.

To the Brazilian Army, for having allowed me to do an academic master's degree within my area of activity, elevating my professional knowledge.

ABSTRACT

UNCERTAINTY QUANTIFICATION AND RELIABILITY ANALYSIS OF EXISTING CONCRETE BRIDGES USING REAL AND UPDATED TRAFFIC LOADS

Author: Fernando Merlim de Oliveira
Advisor: Francisco Evangelista Júnior
Postgraduate Program in Structures and Civil Construction
Brasilia, February of 2023.

This work proposes a method to analyze the design traffic load used in concrete bridges comparing it to real traffic based on uncertainty quantification and reliability structural. As a case study, the Brazilian and American design vehicles were used, and for such, it was considered the verification of the structural safety through the reliability index β. The analyses were applied to bridges with spans of 20, 30, and 40 meters, and the ultimate bending moments were studied. To represent the real traffic, a known database of vehicles was admitted, which makes use of the identification of heavy trucks according to the National Department of Transportation Infrastructure (DNIT), assuming that the bending moments induced by these vehicles follow the same probability density function of the respective weights. In addition, to the analysis at time T=0 when the weighing was taken, verifications were also exposed for the extrapolated vehicle weights for a return period (T) of 15, 50, and 75 years. An extrapolation methodology and Monte Carlo simulations were used to obtain the extrapolated vehicle weights and the respective bending moments. The results indicate that the reliability indexes obtained were lower than the minimum required by international codes, including the value for the reliability index stipulated by AASHTO LRFD and that was used in the specifications of this standard for its calibration. Encourages better inspection practices regarding the weight of vehicles and the necessity for improvements of standards relating to traffic loads and/or bridges. Moreover, regarding traffic loads only, a higher percentage of the characteristic values of the live loads were exceeded in the unfavorable direction, if compared to recommended ABNT standard within the stipulated return period of 50 years.

Keywords: traffic load, structural reliability, bridges, ultimate limit state.

RESUMO

ANÁLISE DA QUANTIFICAÇÃO DA INCERTEZA E CONFIABILIDADE DE PONTES EXISTENTES DE CONCRETO USANDO CARGAS DE TRÁFEGO REAIS E ATUALIZADAS

Autor: Fernando Merlim de Oliveira
Orientador: Francisco Evangelista Júnior
Programa de Pós-graduação em Estruturas e Construção Civil da Universidade de Brasília
Brasília, fevereiro de 2023.

Este trabalho propõe um método para analisar trens-tipo utilizados em pontes de concreto, comparando-os com o tráfego real, baseado na quantificação da incerteza e na confiabilidade estrutural. Como estudo de caso, foram utilizados os trens-tipo brasileiro e americano, e para tanto, foi considerada a verificação da segurança estrutural através do índice de confiabilidade β. As análises foram aplicadas a pontes com vãos de 20, 30 e 40 metros, e foram estudados os momentos fletores últimos. Para representar o tráfego real, foi admitido um banco de dados conhecido de veículos, que faz uso da identificação de caminhões pesados de acordo com o Departamento Nacional de Infraestrutura de Transporte (DNIT), assumindo que os momentos fletores provenientes destes veículos seguem a mesma função de densidade de probabilidade dos respectivos pesos. Além da análise no momento T=0 quando a pesagem foi realizada, também foram expostas verificações para os pesos extrapolados dos veículos para um período de retorno (T) de 15, 50 e 75 anos. Uma metodologia de extrapolação e simulações Monte Carlo foram utilizadas para obter os pesos extrapolados dos veículos e os respectivos momentos fletores. Os resultados indicam que os índices de confiabilidade obtidos são inferiores ao mínimo exigido por normas internacionais, incluindo valor para o índice de confiabilidade estipulado pela AASHTO LRFD e que foi utilizado nas especificações da referida norma para fins de sua calibração. Incentiva-se assim, melhores práticas de inspeção no que diz respeito ao peso dos veículos e à necessidade de melhorias das normas relativas às cargas de trânsito e/ou pontes. Além disso, no que diz respeito apenas às cargas de tráfego, uma porcentagem maior dos valores característicos das ações variáveis foi excedida na direção desfavorável, se comparada com a recomendação da norma da ABNT dentro do período de retorno estipulado de 50 anos.

Palavras-Chave: trem-tipo, confiabilidade estrutural, pontes, estado limite último.

CONTENTS

LIST OF FIGURES

LIST OF TABLES

LIST OF SYMBOLS

Latin Letters

a – location parameter

b – scale parameter

c – shape parameter

dd1 – vector containing the Monte Carlo simulation values referring to the dead load of structural elements

dd2 – vector containing the Monte Carlo simulation values referring to the dead load of guardrails

dd3 – vector containing the Monte Carlo simulation values referring to the pavement

ll – vector containing the Monte Carlo simulation values referring to the live load

f_{ck} – characteristic compressive strength

F_d – design value for Brazilian standard

f_R – marginal probability function of resistance quantity

f_{RS} – joint probability function of resistance and solicitation quantities

f_S – marginal probability function of solicitation quantity

f_x – probability density function

F_x – cumulative density function

G – performance function

I – a function that computes the number of times the performance function is less than zero

k – shape parameter for Gamma distribution

L – static live load effect

L_{iv} – span Length in meters

$M_{AASHTO/F}$ – ultimate bending moment for American standard

M_k – bending moments without load factors

M_n – bending moments obtained in the simulations

M_{NBR} – bending moment without load factors for Brazilian standard

$M_{NBR/F}$ – ultimate bending moment for Brazilian standard

M_{P1} – bending moment induced by a unit load

M_μ – bending moment induced by mean gross weight

M_t – bending moments related only to traffic loads

m_{LP+I} – mean bending moment referring to the dynamic effect and static live loading

n – number of lanes

n_{MC} – numbers of values generated by Monte Carlo simulation

N – number of trucks for a determined return period

P – analysis factor

P_{axle} – weight per axle

p_f – failure probability

Q – design value for American standard

Q_i – characteristic value of the load according to American standard

R – resistance quantity

S – solicitation quantity

T – return period

u - random number generated, variable and uniform between 0 and 1

V – coefficient of variation

X – variable that extrapolation is desired to know

x_r – vector of random variable referring to the resistance quantity

x_s – vector of random variable referring to the solicitation quantity

Z – the inverse of the cumulative probability function of the standard normal distribution

Greek Letters

α - percentage quantity of the probability distribution

β – reliability index

$β_T$ – target value for reliability index

Γ – Gamma function

γ – load factors, incomplete Gamma function

η – load modifier

θ – scale parameter for Gamma distribution

λ – the ratio between the mean bending moment and resistant bending moment

μ – mean of the probability distribution

$μ_M$ – mean of the bending moments

σ – standard deviation of the probability distribution

Φ – cumulative probability function of the standard normal distribution

φ – mixing parameter

$Ψ_{0j}$ – reduced combination value

ω – ratio between the mean and design value

LIST OF ABBREVIATIONS

AASHTO - American association of state highway and transportation officials

ABCR – Brazilian association of highway concessionaires

ABNT – Brazilian association of technical standards

ACI – American concrete institute

ADTT – average daily truck traffic

CDF – cumulative density function

CIA – additional impact coefficient

CIV – vertical impact coefficient

CNF – number of lanes coefficient

CONTRAN - national transit council

DNIT - national department of transportation infrastructure

fib - international federation for structural concrete

FORM – first order reliability method

GVW – gross vehicle weight

EGVW – extrapolated gross vehicle weight

ICDF – inverse cumulative density function

IM – dynamic load allowance

LRFD - load and resistance factor design

MLL – maximum legal load

NBR – Brazilian technical standard

PDF – probability density function

PMC – probabilistic model code

SORM – second order reliability method

ULS – ultimate limit state

WIM – weight in motion

CHAPTER 1 – INTRODUCTION

1.1 Contextualization and State of Art

Structural designs require updated standards to reflect reality since the design traffic loads become outdated in the face of changes in the weight and volume of traffic on highways. Traffic, consisting of vehicles and pedestrians, originates forces with static and dynamic effects, which the current standards around the world try to represent these loads through models with its design vehicles. In this way, Šavor and Novak (2015) claim that the evaluation of existing bridges based on these standards may show the need for rehabilitation or even replacement of these structures.

The analysis focused on heavy traffic vehicle loading is justified by Ramesh Babu et al. (2018), whose work asserts that the service life of a bridge is most affected by heavy traffic loads and their respective loading effects on the structure. Also, it states that the new generation of American regulations and from many countries have reliability as the basis for ensuring adequate safety, based on extrapolation methods, just like the one proposed in this work. Analyses using heavy loads are argued for by Khan et al. (2021) who state that infrastructure components such as bridges are often subjected to overloads while experiencing deterioration with age and Pais et al. (2021) who claim that this loading makes the costs of road constructions and their respective rehabilitations higher.

Mandić Ivanković et al. (2017) brought the need to evaluate the effect of each element on the total condition of bridges by determining their impact on structural safety, traffic safety, and durability. The probabilistic evaluation was done using Weight-in-Motion (WIM) vehicle data to develop the structural reliability of these structures over a specified lifetime. The use of this type of truck weight data collection is noted by Gonçalves et al. (2022) who pointed out the monitoring of traffic weight by WIM as being useful for management decisions and may have applicability in the calculation of influence lines and damage detection, as well as Bosso et al. (2019) who used WIM to describe a method for identifying overloaded truck weights and travel patterns on the BR-361 highway in Brazil.

To generate sufficiently large samples capable of estimating the effects of traffic loading on bridges for long periods, many recent studies have adopted the Monte Carlo simulation approach (O'Brien et al., 2015; Caprani et al., 2016; Lu et al., 2017). Furthermore, it has been shown that such computational simulation aimed at the long term can result in high extrapolation accuracy (O'Brien et al., 2015).

Several studies have been done over the years to adapt the live loads of the standards to the real traffic conditions in bridges. It can be pointed out relevant works such as Nowak et al. (1993), Nowak (1993), Nowak (1999), Nowak and Szerszen (2000) as well as Nowak and Rakoczy (2013), which generally sought to develop methods to obtain live loads for bridge standards based on the application of structural reliability and probabilistic theories, including some of them, by using statistical parameters obtained from WIM. In addition, these studies showed the importance of the development of a live load model is essential for a rational bridge design and/or evaluation standard.

Some authors have already demonstrated that ABNT NBR 8681 (2003) and ABNT NBR 7188 (2013), for the design of reinforced concrete bridges, may not fully represent what is obtained when considering the real and updated traffic of heavy vehicles on highways. These authors obtained similar results to those of this dissertation, evidencing in this work, the incompatibility of the reliability indexes concerning standards or codes. This is illustrated by El Debs et al. (2005) who characterized the incompatibility of some vehicles with certain classes of Brazilian bridges, Ferreira et al. (2008) who created equations to regulate the traffic of cargo vehicles, Santos and Pfeil (2014) who proposed a live load model compatible with the characteristics of the current vehicular traffic on bridges in Brazil, Rossigali et al. (2015) who expressed that the static effects of traffic may not adequately reproduce the real traffic of heavy vehicles, Stucchi and Luchi (2015) that suggested a percentage increase in the Brazilian design vehicle that was adopted in ABNT NBR 7188 (2013), Portela (2018) who proposed a different design vehicle load and Braz (2019) who demonstrated that the actual traffic generated probabilistic fatigue factors higher than the calculated fatigue factors as demanded by the Brazilian standard, being an additional indication for the inadequacy of the live load of the standard when compared to the observed traffic.

It is noticeable that Brazil has presented an evolution in road transport. This evolution has caused an increase in the loads to be transported, which results in concern regarding the capacity of existing bridges and future constructions. This work is justified by the fact that the demand for road transport increases year after year and, consequently, the traffic of heavy vehicles on the highways, as verified by the index of heavy vehicles flow created by the Brazilian Association of Highway Concessionaires (ABCR), which amplifies the chances of structural problems in existing bridges.
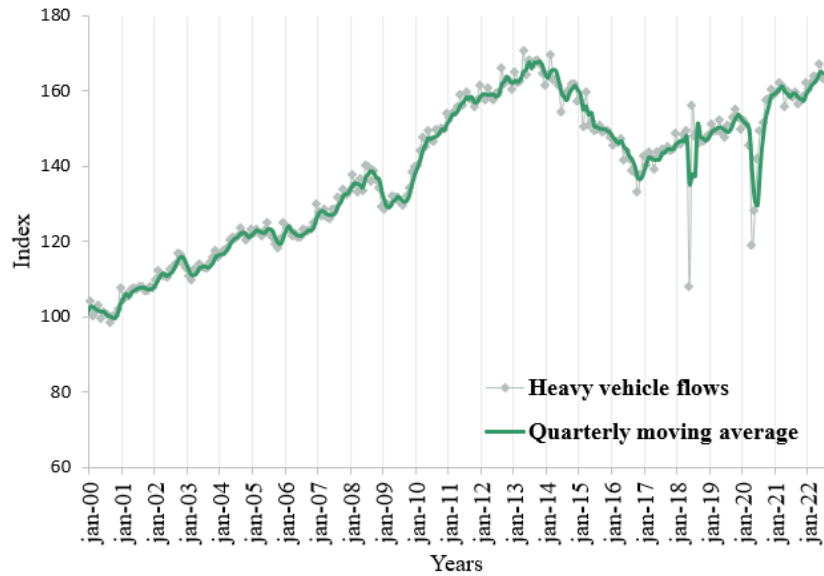
Figure 1.1 – Brazilian heavy vehicle flow. Source: ABCR (2022).

Moreover, it can be noted that in Brazil there are approximately 137,000 bridges, viaducts, and footbridges, of these 6,612 are under the responsibility of the National Department of Transportation Infrastructure (DNIT) and at least 3,351 are in situations that vary from precarious to poor state of conservation (Timerman, 2015).

The overloading of bridges is a factor that can lead these structures to collapse, as shown by Vitorio (2007) who listed several constructions that were compromised, highlighting the bridge with a span of 7m over the Riacho da Barra on the PE-280 highway, which collapsed in 2022, due to overloading as a major factor.

This dissertation aims to verify the reliability of concrete bridges, considering the characteristics of real vehicles passing over the Brazilian highways for models based on the design vehicles recommended by ABNT NBR 7188 (2013) and AASHTO LRFD (2020). To this end, a maximum load effect was used in which the bridges were subjected to a 75-year return period (T), a period analogous to that stipulated by the AASHTO LRFD (2020), based on the extrapolation method proposed by Nowak (1999) and Monte Carlo simulations. Comparatively, the analysis was also done for a return period of 50 years, the reference period of ABNT NBR 8681 (2003), and in addition a return period of 15 years, to get an idea of what happens around T=0.

According to Ghosn et al. (2016), reliability theory has been used over the past decades as a widespread tool in the field of structural engineering to evaluate the safety and performance of structures, such as bridges. As commented by Wang et al. (2018), such application is possible to be done in the sense of using a structural reliability method based on the use of probability

distribution functions considering the uncertainty of external loads, focusing mainly on the case of this work, on traffic loads. Moreover, authors such as Kala (2019) and Alampalli et al. (2021) used the computation of structural reliability indexes based on the probabilities of failure within the analyses performed in their research on bridges. Therefore, this analysis may contribute to designers and road regulatory agencies, regarding the decision of whether to authorize certain vehicular configurations to travel on certain stretches of highways, as well as ABNT (Brazilian National Standards Organization), concerning possible improvements of standards.

1.2 Objective

The goal of this dissertation is to consider measuring actual traffic loads and frequency to extrapolate traffic data on gross vehicle weights to return periods of 15, 50, and 75 years, to evaluate the reliability of bridges according to current and extrapolated data, based on the maximum bending moments in the girders of the concrete bridges studied.

1.2.1 Specific Objectives

The specific objectives are:

i. Uncertainty quantification of bending moments using Monte Carlo simulation and an extrapolation method for vehicle weights;

ii. Verification of the best Probability Density Function for the maximum bending moments found;

iii. Analyze standard design vehicles from a reliability standpoint when compared to real traffic for return periods of 15, 50, and, 75 years, to check whether the design recommendations are adequate given the variability observed in practice;

iv. Consider current traffic loads and frequency data as pointed out by Rossigali et al. (2015), and extrapolation of gross vehicle weight based on the method developed by Nowak (1999);

v. Creation of a ratio λ such that it is possible to stipulate the failure probability of similar bridges as those studied;

vi. Compare the reliability indexes obtained, taking the ABNT NBR 7188 (2013) and AASHTO LRFD (2020) as a reference of resistance quantity; and

vii. Compare the conservatism of the Brazilian and the American standards about the use of their respective load factors.

1.3 Dissertation Organization

This dissertation has five chapters including this introductory one.

Chapter 1 is an introduction to the dissertation and presents the objectives of this work, besides the main motivations.

Chapter 2 presents a bibliographic review of the concepts and premises of the standards that were studied to support the proposed method for verifying standard design vehicles.

Chapter 3 presents a method for analysis of existing concrete bridges, taking into consideration the Brazilian and American design vehicles as a case study and real and updated traffic load. It observed return periods of 15, 50, and, 75 years, to check whether the design recommendations are adequate given the variability observed in practice.

Chapter 4 provides the uncertainty of the quantification of the bending moments, to show the histograms, and probability distributions that best fit and quantify values of the bending moments of the analyzed standards, besides the structural reliability analysis, focused on the β index.

Chapter 5 contains the conclusions and recommendations for future works.

CHAPTER 2 – BACKGROUND

This chapter presents the preliminary context for applying the proposed methodology, whose objective is to present the main premises of the standards in study and concepts that must be observed for understanding.

2.1 Ultimate Limit States

According to ABNT NBR 8681 (2003), limit states are defined as states from which the structure presents inadequate performance for construction. When it comes to Ultimate Limit State (ULS), these are defined as states that determine the loss of equilibrium, rupture, the excessive plastic strain of the materials, or instability of the structure, making it unusable for reasons of exhaustion of the load carrying capacity or safety risks.

According to Ferreira et al. (2008), in the case of the ultimate limit state, the maximum effect of loading during the structure's service life is of fundamental interest. However, since traffic data on bridges is often limited, it is necessary to predict the maximum bending moment for longer periods.

2.2 Loads

The loads induce stress and strains in structures, as defined in ABNT NBR 8681 (2003). These can be classified as dead, live, and exceptional. According to ABNT NBR 7187 (2020), dead loads are defined as those whose intensities can be considered constant throughout the life service, such as pavement, and guardrails, which were objects of consideration in the case studies analyzed. On the other hand, the live loads have variable nature, such as traffic load.

2.2.1 AASHTO LRFD (2020)

According to AASHTO LRFD (2020), traffic loading for bridges is defined as a combination between pre-established vehicles referred to as design truck or design tandem, and a uniformly distributed load referred to as design lane.

The vehicle defined for the design truck features 3 axles (named HS20-44), with the front axle being approximately 35 kN and the other axles approximately 145 kN, while the vehicle defined for the design tandem consists of a pair of axles of approximately 110 kN each and spaced by 1.20 meters with a transverse distance between wheels of 1.80 meters, as Figure 2.1.
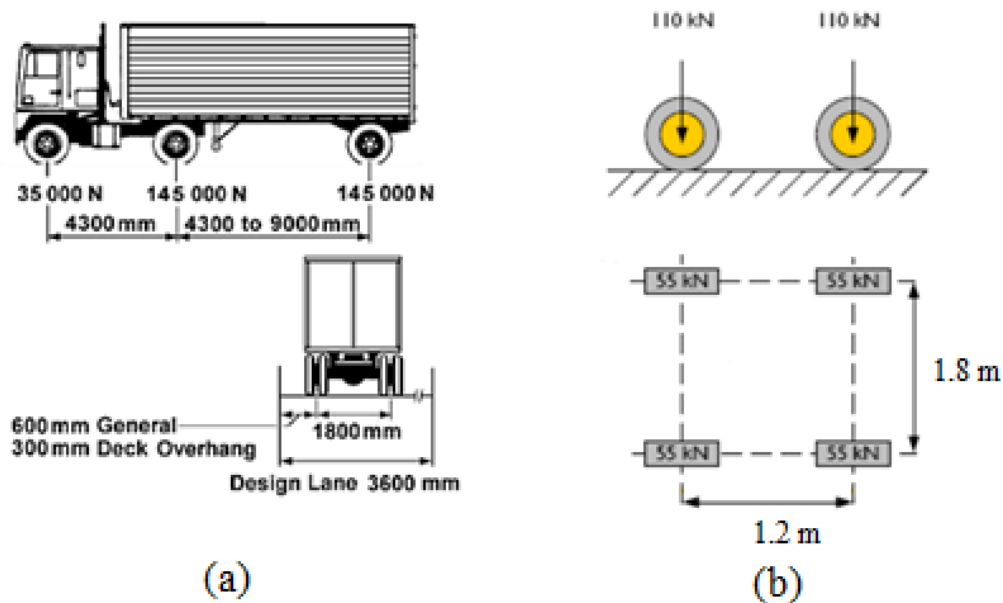
Figure 2.1 - Design vehicles for AASHTO LRFD (2020): (a) design truck; (b) design tandem. Source: AASHTO (2020).

In combination with the above-mentioned vehicles, the American standard defines that a uniformly distributed load of 9.34 kN/m must be applied along the longitudinal direction, called design lane load. Transversely, this load is distributed over a width of 3.00 meters. The force effect of the traffic load is assumed to be the greater of the following:

    i. The effect of design tandem combined with design lane load;

    ii. The effect of design truck combined with design lane load;

    iii. The combination of 90% of the effect of two HS20-44 vehicles (spaced at least 15.24 meters apart - between the front axle of one truck and the rear axle of another) with 90% of the design lane load. The 145.15 kN wheelbase of each truck should be 4.27 meters.

Like the ABNT NBR 7188 (2013), the AASHTO LRFD (2020) also provides a load increase coefficient for design vehicles, called Dynamic Load Allowance (IM). It is expressed that the static loads of design truck or design tandem vehicles must be increased by the percentage expressed in Table 2.1:

Table 2.1 - Dynamic Load Allowance (IM) of AASHTO LRFD (2020)

Limit State	IM
Fatigue and Fracture	15%
Others	33%

For the ultimate limit state case, an IM of 33% is used, and it should be noted that the impact load is not applied to distributed traffic loads.

2.2.2 ABNT NBR 7188 (2013)

According to ABNT NBR 7188 (2013), a design vehicle is defined such that it assumes any position across the roadway with the wheels in the most unfavorable position, including shoulders. The design vehicle, in this case, is the TB-450, defined as being a 450 kN vehicle with six wheels, with the equivalent static load P of each wheel, equivalent to 75 kN, positioned on three load axles spaced 1.50 meters apart, occupying an area of 6x3m, and surrounded by a distributed load p = 5 kN/m², as Figure 2.2:
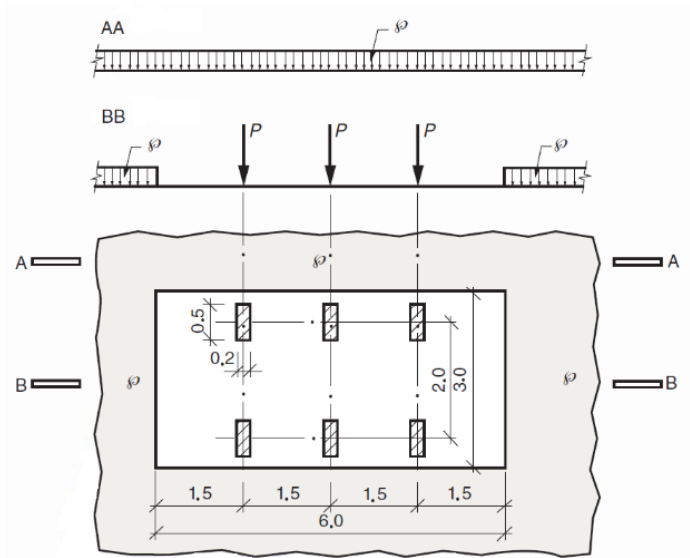
Figure 2.2 - Design Vehicle TB-450 of ABNT NBR 7188 (2013). Source: ABNT NBR 7188 (2013).

In addition to the design vehicle, the ABNT NBR 7188 (2013) defines Vertical Impact Coefficient (CIV), Number of Lanes Coefficient (CNF), and Additional Impact Coefficient (CIA). The impact load is the product of these portions.

a) CIV is determined as:

$$CIV = \begin{cases} 1.35, \text{ for spans less than 10 m} \\ 1+1.06(\dfrac{20}{L_{iv} + 50}) \end{cases} \tag{1}$$

Where L_{iv} is the span in meters, depending on the type of structure.

b) CNF as:

$$CNF = 1 - 0.05(n - 2) > 0.9 \tag{2}$$

Where n is the integer number of lanes to be loaded on a transversely continuous deck, not including shoulders.

c) The CIA as a recommendation for the regions of structural joints:

22

$$CIA = \begin{cases} 1.25, \text{ for concrete bridges} \\ 1.15, \text{ for steel bridges} \end{cases} \tag{3}$$

Therefore, ABNT NBR 7188 (2013) defines that the static loads P of each wheel and the distributed load p should be increased by multiplying them by the product of the coefficients obtained by Equation (1), (2) e (3).

2.3 Combinations

It is necessary to determine the design quantities, which is done by combining the loadings and their respective load factors, as each standard prescribes.

2.3.1 American Standard

AASHTO LRFD (2020) presents several load factors of the most varied possible loadings to be represented in a bridge, where the total increased load Q is given by:

$$Q = \sum \eta_i \gamma_i Q_i \tag{4}$$

Where η_i is the load modifier, γ_i is the load factor and Q_i is the characteristic value of the load. The factor η from Equation (4), is a function of ductility, redundancy, whose meaning is the ability of a bridge structural system to be able to support loads after damage or failure of one or more of its members, and, the operational importance. As an object of study, it can be considered $\eta=1.00$ for the cases of conventional or typical bridges.

The load factors γ must be chosen to produce the maximum effect of the loads. In load combinations where one effect reduces the other, the minimum value applies to the load that is reducing the effect. The load factor (maximum or minimum) from Table 2.2 that produces the most critical combination should be chosen for dead load effects.

Table 2.2 - Load Factors of AASHTO LRFD (2020)

Type of Load	γ	
	Maximum	Minimum
Dead load of structural components and nonstructural attachments	1.25	0.90
Dead load of wearing surfaces	1.50	0.65

Source: Adapted from AASHTO LRFD (2020).

The load factor γ for the live load is a function of the limit state in which the verification is desired. In this case, for the Ultimate Limit State, the state called by the American standard as Strength I was considered, whose principle is the basic combination of loads related to the common use of live loads without wind load. For such, $\gamma=1.75$.

2.3.2 Brazilian Standard

According to ABNT NBR 6118 (2014), a loading is defined as a combination that has non-negligible probabilities of acting simultaneously on the structure during a pre-established period.

The combination of loads must be done so that the most unfavorable effects for the structure can be determined, and the verification for the ultimate limit state must be performed as a function of the ultimate combinations. To obtain the most unfavorable bending moment, the normal ultimate combination should be performed, given by Equation (5), in which are included the dead loads and the live loads with their characteristic values, according to ABNT NBR 8681 (2003).

$$F_d = \sum_{i=1}^{n} \gamma_{gi} F_{gik} + \gamma_q \left(F_{q1k} + \sum_{j=2}^{n} \Psi_{0j} F_{qjk} \right) \tag{5}$$

Where F_d is the design value, the result of the load factors; γ_{gi} is the load factor for dead loads; F_{gik} is the characteristic value of the dead load; γ_q is the load factor for live loads; F_{q1k} is the characteristic value of the main live load; Ψ_{0j} is the reduced combination value of each of the other live loads; F_{qjk} is the characteristic value of the secondary live load. According to ABNT NBR 8681 (2003), for bridges in general and normal ultimate combinations, the following load factors are used $\gamma_g = 1.35$ for dead loads and $\gamma_q = 1.50$ for live loads.

2.4 Structural Reliability

Structural reliability is the ability of a structure to attain its design purposes in a specified period (design life). More specifically, reliability is the probability that the structure will not fail to perform its function over the specified design life.

In a simplified way, can be described by only two quantities, a solicitation quantity S, and a resistance quantity R. In general, the quantities R and S are modeled as random variables (two-dimension presentation), thus being able to evaluate the probability of the event S>R, a probability denoted as failure probability p_f, i.e., the probability of exceeding some limit state. Note that the quantities $R(x_r)$ and $S(x_s)$ can also be vectors of random variables x_r and x_s.

Encompassing these concepts, a performance function can be defined, such that G(R,S)=R-S. The performance function presented can then have a domain associated with failure, that is, G(R,S)<0, as well as another domain associated with safety, that is, G(R,S)>0.

$$p_f = P(R - S < 0) = P(G(R,S) < 0) \tag{6}$$

In a probabilistic approach to structural safety, it is sought that the probability of failure is less than a value accepted as the maximum permissible, or target value, such that it varies for each limit state.

Let $f_R(r)$, be the marginal probability function of R, $f_S(s)$, the marginal probability function of S and f_{RS}, the joint probability function of variables R and S, and the probability of failure can be represented by a volume as represented by Figure 2.3(a) and quantified by Equation (7).

$$p_f = \iint_{G<0} f_{RS}(r,s)\,dr\,ds \tag{7}$$

The evaluation of this integration is usually difficult to perform. Numerical methods and other approximations are commonly used to evaluate the integral, but the accuracy may not be adequate (Nowak and Collins, 2012). Therefore, the probability of failure is determined through indirect methods such as First Order and Second Order reliability methods (FORM and SORM) and Monte Carlo Simulations (Nowak and Collins, 2012; Melchers and Beck, 2018).
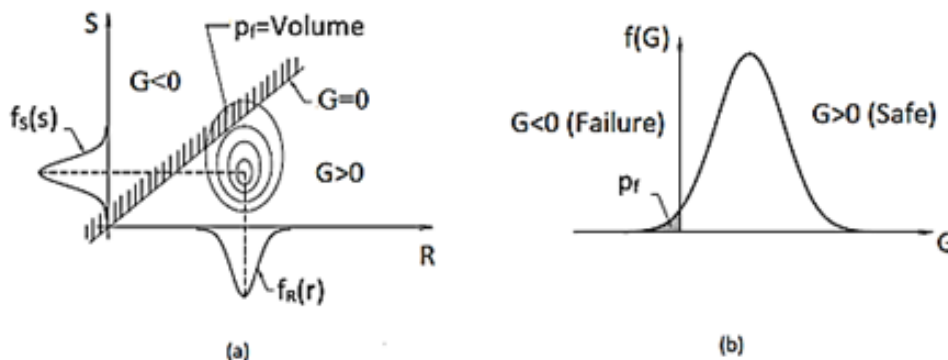

Figure 2.3 - Reliability problem (a) Performance function G; (b) Probability density function of G.

The FORM method represents the limit state equation by a linear function, allowing the consideration of statistical information specific to random variables, such as probability

distributions and correlation between the variables. The SORM method also allows the use of the statistical information of the random variables but represents the limit state equation as quadratic surfaces.

In FORM and SORM methods, the p_f is estimated through a reliability index β which is the shortest distance from the origin of the equivalent non-correlated standard normal input variables to the surface of the limit state function (G=0). In Monte Carlo Methods, the probability of failure can be obtained through one or more probability density functions, which can be derived from experimental data or theoretical models.

Thus, in addition to the analytical solution for calculating p_f, given by Equation (7), the probability of failure can be obtained from a function I that computes the number of times G(R,S)<0, as shown in Equation (8), from the numbers generated by Monte Carlo simulation n_{MC}.

$$p_f = \frac{1}{n_{MC}} \sum_{i=1}^{n_{MC}} I[G(R_i, S_i) < 0] \tag{8}$$

This equation is an estimation of the probability of failure given in the integral of Equation (7). The resultant probability estimated value is also a random variable with mean and standard deviation. However, the standard deviation of the estimated probability decreases with the increase of the number of simulations n performed for Equation (8).

Based on the evaluation of p_f, the quantity reliability index β can be determined using the relation:

$$\beta = -\Phi^{-1}(p_f) \tag{9}$$

Where, Φ^{-1} is the inverse of the standard normal Cumulative Probability Function (CDF).

For structural reliability analysis, the amount of resistance R was taken for a deterministic ULS value, as a function of the applied standard, while the solicitation quantity S, encompasses the uncertainties around the input parameters of the phenomenon under study from the consideration of the respective probability density functions.

CHAPTER 3 – PROPOSED METHOD

This chapter presents the methodology used to apply a design vehicle analysis method about real and updated traffic load for existing reinforced concrete bridges. For this application, the Brazilian and American design vehicles were observed for the return periods of 15, 50, and 75 years, based on the respective regulatory considerations necessary for verification. The problem consists in analyzing whether the design recommendations are adequate given the variability observed in practice.

3.1 Method Overview

To summarize the proposed methodology, a flowchart of the steps to be followed was created (Figure 3.1), whose final objective was analyze whether the design vehicle of a given standard satisfies the specificities of actual traffic in terms of structural reliability.

First of all, the choice of the bridge geometry to be analyzed must be made, in addition to the selection of the actual vehicles, where it is recommended to choose the heaviest and most frequent ones. After the characterization of the relative frequency of the adopted vehicles, the Probability Density Function (PDF) of the weights of these trucks must be known, to obtain the extrapolation straight line from some method such as Nowak (1999). The compilation of this statistical data is done to implement the structural simulation in software, to obtain the mean of the bending moments in a given pre-established return period T. From this step, the uncertainty quantification of the bending moments can be obtained from Monte Carlo simulations, assuming that the bending moments induced by each chosen vehicle, follow the same PDF of the respective truck weight and also the same coefficient of variation. Finally, a structural reliability analysis is done using the β index.
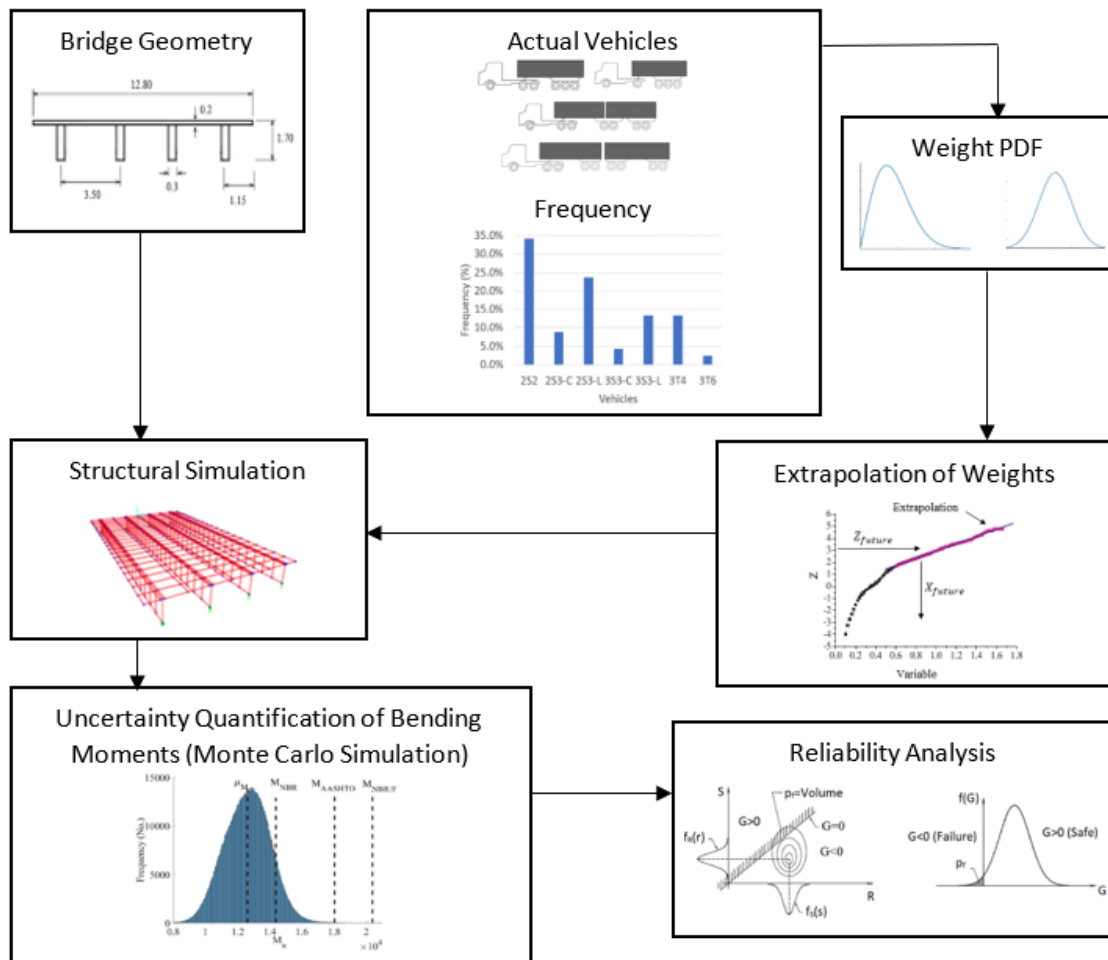
Figure 3.1 - Flowchart of the proposed method.

3.2 Bridges Geometry

The choice was made for the geometry of simply supported bridges, taking as parameters spans 20 m, 30 m, and 40 m. The deck width is 12.80 m and the deck slab is integrated with four girders.

Concrete with characteristic compressive strength (f_{ck}) equal to 30 MPa was used for both girders and slab. For the specific weight of the reinforced concrete, it was followed that recommended by ABNT NBR 6118 (2014), which determines that the value of 25 kN/m³ can be adopted.

In addition to the dead load, it was used guardrail loads of 5.80 kN/m, referring to concrete elements with a cross-sectional area of 0.23 m² (0.4 x 0.58 m) and paving load of 1.20 kN/m² referring to a thickness of 5 cm, considering the specific weight equal to 24 kN/m³.

Table 3.1 - Adopted Bridges

Cross Section [2]	Longitudinal Layout

3.3 Actual Vehicles and Frequency Adopted

The commercial vehicles that pass over on Brazilian roads are defined in the Table of Vehicle Manufacturers (DNIT, 2012). Each type of vehicle has a different composition of its axles, which culminates in a division of vehicles by class.

Each of the axles of these vehicles has a certain Maximum Legal Load (MLL), established by the resolution of the National Transit Council (CONTRAN) No. 210/2006, which can be placed on each axle. Figure 3.2 shows the respective maximum loads for single axles (those whose centers are in a vertical transverse plane) and tandem axles (those consisting of an integral suspension assembly), being for the single wheel single axle (60 kN), double wheel single axle (100 kN), double tandem axle (170 kN), and triple tandem axle (255 kN).
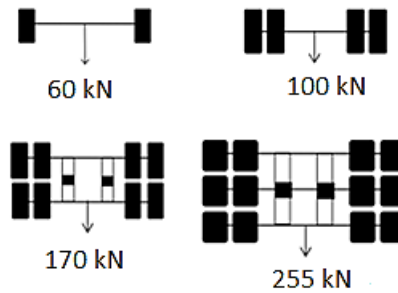
Figure 3.2 - Maximum Legal Load (MLL) for each axle type. Source: DNIT (2012).

Although there is no consensus regarding the nomenclature that should be adopted nationwide, DNIT suggests an identification represented by a code composed of up to two numbers, interspersed by a letter. The first number indicates the number of axles of the tractor unit, while the second number indicates the number of axles of the towed units. The main codes are described as established:

- nSm: a mechanical horse with n axles carrying a towed unit of the semitrailer type (S) with m axles;
- nIm: the letter I indicate that the m axles are spaced more than 2.4 m apart, increasing the possible load;
- nCm: platform truck with n axles carrying a trailer coupled with m axles;
- nTm: a mechanical horse with n axles carrying two or three towed units of the semitrailer type (T), which together total m axles. The total number of axles of the train is given by n+m.

Some vehicles still take the denomination of short (C) and long (L), due to the variability of the distance between axles. Next, Figure 3.3 shows the vehicles used in this work with their respective nomenclature, the distance between axles, and the value of maximum permitted Gross Vehicle Weight (GVW).
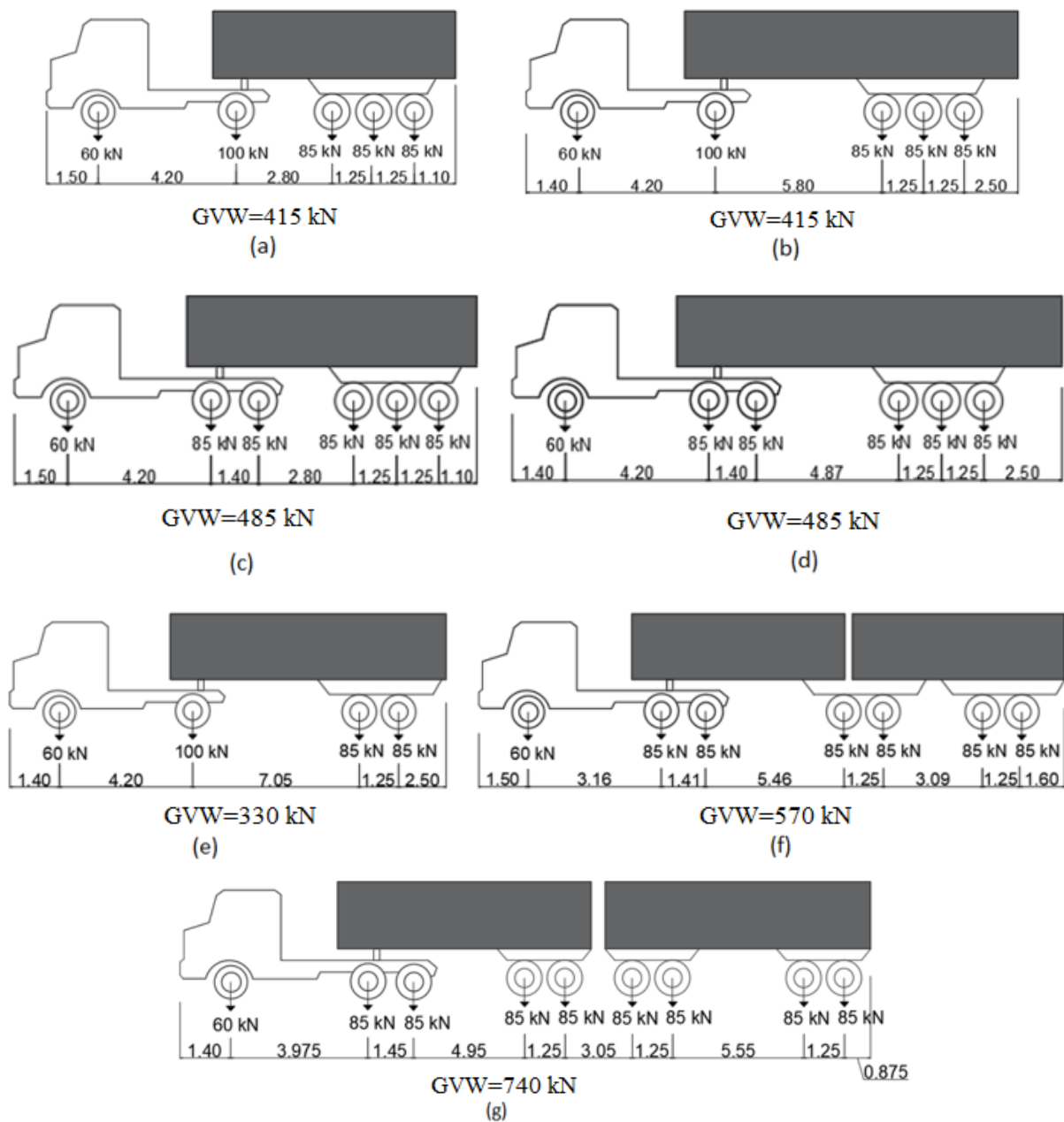
Figure 3.3 - Categorized vehicles: (a) 2S3-C; (b) 2S3-L; (c) 3S3-C; (d) 3S3-L; (e) 2S2; (f) 3T4; (g) 3T6.

    The database used as a source in this work was the same made by Rossigali et al. (2015) derived from elements of federal and private Brazilian highways (Bandeirantes Highway-SP 348, BR 116, and BR 277) and used by Moura (2019). This hybrid database represents traffic from the south and southeast regions of Brazil, obtained from WIM data over the years 2008 to 2011, generating the traffic composition pointed out in Figure 3.4(a), being adopted in this work the vehicles 2S2, 2S3-C, 2S3-L, 3S3-C, 3S3-L, 3T4, and 3T6, justified among those more frequent and heavier, whose relative frequencies are in Figure 3.4(b).

31

Figure 3.4 - Collected relative frequency on Brazilian highways presented by Rossigali et al. (2015): (a) all vehicles; (b) adopted vehicles in this dissertation.

The transverse dimensions adopted for the vehicles in Figure 3.3, were the same as those used by Rossigali et al. (2015) in Table 3.2.

Table 3.2 - Axle Transverse Spacing for Categorized Vehicles

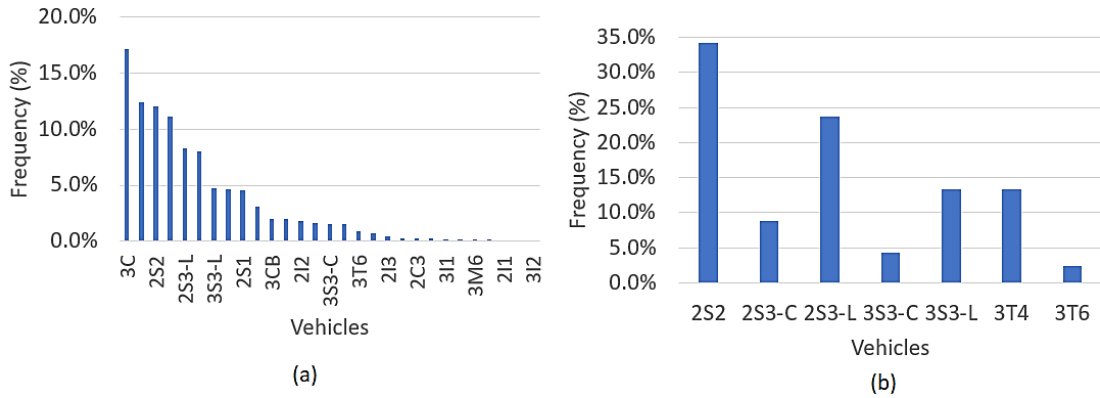| Vehicle	Axle 1	Axle 2	Axle 3	Axle 4	Axle 5	Axle 6	Axle 7	Axle 8	Axle 9
2S2	2.05	1.85	1.90	1.90	1.90	-	-	-	-
2S3-C	2.05	1.85	1.90	1.90	1.90	-	-	-	-
2S3-L	2.05	1.85	1.90	1.90	1.90	-	-	-	-
3S3-C	2.05	1.85	1.85	1.90	1.90	1.90	-	-	-
3S3-L	2.05	1.85	1.85	1.90	1.90	1.90	-	-	-
3T4	2.05	1.85	1.85	1.90	1.90	1.90	1.90	-	-
3T6	2.05	1.85	1.85	1.90	1.90	1.90	1.90	1.90	1.90

Source: Adapted from Rossigali et al. (2015).

3.4 Weight PDF

The results were analyzed to observe if the current design vehicle in the ABNT NBR 7188 (2013) satisfies the ULS when compared to the real vehicles that pass over the highways, cataloged by DNIT, both for their current weights (T=0), as for the return periods of 15, 50 and 75 years. It is assumed, in this proposed method, that the bending moments induced by the vehicles, follow the same PDF of the respective weights. All PDFs presented in Table 3.3, as well as the mean μ, standard deviation σ, and coefficient of variation V, were based on the results from Rossigali et al. (2015) who determined the curve best fitting the data from the frequency histograms of federal highways from WIM data. The data in Table 3.3 are similar to those found for WIM measurements presented by Portela (2018) on the Fernão Dias highway, in the state of São Paulo over the years 2015 to 2017.

Table 3.3 - Statistical Parameters of the (T=0) Gross Vehicle Weights

Vehicle	μ (kN)	σ (kN)	V	PDF
2S2	198.00	43.10	0.218	Gumbel
2S3-C	403.00	51.40	0.128	Double Exponential
2S3-L	366.00	76.00	0.208	Minimum Extreme Value – Type II and Rayleigh (Bimodal)
3S3-C	452.00	27.40	0.061	Double Exponential
3S3-L	450.00	52.60	0.117	Minimum and Maximum Extreme Value – Type II (Bimodal)
3T4	552.00	45.20	0.082	Double Exponential
3T6	709.00	53.00	0.075	Minimum Extreme Value – Type II

Source: Adapted from Rossigali et al. (2015).

However, it should be mentioned that for the return periods of 15, 50, and 75 years, the means and standard deviations considered for each vehicle are those calculated according to the extrapolation process explained in the next section 3.5.

To support the hypothesis that the same PDF of the vehicle weights can be adopted for the bending moments, Table 3.4 shows the linearity between both comparing the bending moment induced by a unit load of each vehicle M_{P1} and the bending moment induced by mean gross weights of each vehicle M_μ (Table 3.3), for $\ell 20$, through a relation R such that it equal to $(M_\mu / M_{P1})/\mu$.

Table 3.4 – Relation R between bending moments

Vehicle	M_{P1} (kNm)	M_μ (kNm)	R
2S2	2.28	450.24	1.00
2S3-C	2.84	1167.16	0.98
2S3-L	2.45	914.77	0.98
3S3-C	2.8	1236.85	1.02
3S3-L	2.47	1081.44	1.03
3T4	2.11	1157.73	1.01
3T6	1.59	1179.62	0.96

Since the R ratios are approximately equal to 1.00, then the hypothesis can be adopted.

3.5 Gross Vehicle Weight Extrapolation Method

In this dissertation, it is emphasized the method developed by Nowak (1999) to obtain the extrapolations of the gross weights of the vehicles. In his work, extrapolations of the bending moments were obtained based on the Normal Probability, having as the central idea that its upper tail of the cumulative probability distribution is adjusted to a normal distribution. Nowak (1999) characterized that, in general, the trucks have this behavior of a normal distribution for the upper tail of the distribution.

Nowak (1999) calculated the bending moments for each truck in his survey considered, and then extrapolated them. This procedure indicates tendencies for longer periods than the one measured, furthermore is the method used by other researchers for the development of live loading, such as Hwang and Koh (2000), Ferreira et. al (2008), Portela (2018) and Moura (2019). In a slightly different way from Nowak (1999), in this work, the gross vehicle weights were first extrapolated to obtain the maximum bending moments by structural simulations, as also done by Ferreira et. al (2008) and Moura (2019). This allows a computational gain, since it is only necessary to perform a single structural simulation for each span, thus obtaining the mean of the maximum bending moments, to subsequently quantify the uncertainty according to section 3.8.

From the gross vehicle weight CDF, the data is plotted on a normal probability paper, whose property is to have the graphical representation of Z (inverse of the standard normal CDF) as a function of X (random variable that extrapolation is desired to know, in this case, the gross vehicle weights). A basic feature of probability paper is that any series of data that is described by the same type of distribution as the paper is represented by a straight line.

This straight line obtained from the upper tail of the CDF when plotted on a normal probability paper would be the extrapolation line used to obtain future projections (X_{future}). Thus, to obtain X_{future} for a certain return period (in years), the number of future trucks, denominated N, is used from the Average Daily Truck Traffic (ADTT) values, as expressed in Table 3.5.

Table 3.5 - Average Daily Truck Traffic (ADTT) and Number of Trucks N

Vehicle	ADTT	N (15 years)	N (50 years)	N (75 years)
2S2	274	1,498,873	4,996,243	7,494,365
2S3-C	70	385,675	1,285,583	1,928,375
2S3-L	189	1,036,814	3,456,048	5,184,072
3S3-C	34	187,829	626,096	939,144
3S3-L	106	582,269	1,940,897	2,911,346
3T4	106	581,017	1,936,723	2,905,085
3T6	19	106,436	354,788	532,182

Source: Adapted from Moura (2019).

The corresponding cumulative probability p for the number of vehicles N, can be estimated according to $p = {1}/{N}$. Thus, the extrapolated mean gross weight (μ), denoted by the random variable X_{future} is estimated through the intersection of the inverse of the standard normal CDF (Φ^{-1}) on the vertical scale, such as $Z_{future} = -\Phi^{-1}(1/N)$, with the extrapolation line obtained from the upper tail of the CDF, as shown in Figure 3.5.
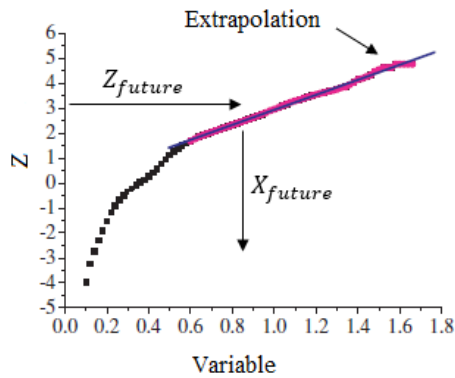
Figure 3.5 - Extrapolation of gross vehicle weight by Nowak's method (1999).

The extrapolation straight lines for each vehicle, in this dissertation, are the same from a dataset of Rossigali et al. (2015) and used by Moura (2019). It was obtained the mean gross weights of the vehicles and their respective standard deviations for the stipulated return periods of 15, 50, and 75 years. The standard deviation σ is given by the slope of the straight line.

Since the extrapolation requires ADTT to be known and since each vehicle has its weighing, i.e., each vehicle has its CDF, this process results in a different mean for each truck and each return period, given that Z changes for each case.

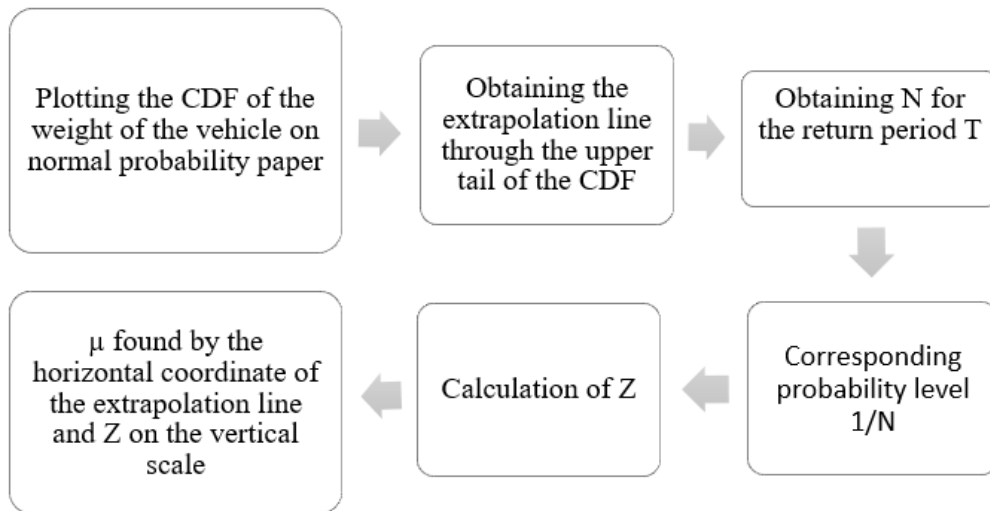Figure 3.6 – Flowchart of extrapolation by Nowak's method (1999).

After determining the Extrapolated Gross Vehicle Weight (EGVW), the weight per axle is determined from the portion by the MLL of the respective axle, according to Figure 3.2. In this way, the weight per axle is given by Equation (10), as done by Ferreira et al. (2008).

$$P_{axle} = \frac{MLL_{axle}}{\sum MLL} EGVW \qquad (10)$$

35

The vehicle extrapolation parameters, considering the return periods of 15, 50, and 75 years are expressed in Table 3.6.

Table 3.6 - Statistical parameters of the gross weights found in the extrapolations

Vehicle	$Z=mx+b$		Z_{15} years	Z_{50} years	Z_{75} years	μ_{15}[1] years	μ_{50}[1] years	μ_{75}[1] years	σ[1]
	m	b							
2S2	0.0085822	0.370966	4.835	5.069	5.145	606.55	634.65	642.77	116.52
2S3-C	0.0079872	1.921159	4.557	4.804	4.884	811.08	841.99	852.06	125.20
2S3-L	0.0183318	10.13949	4.761	4.998	5.075	812.81	825.75	830.00	54.55
3S3-C	0.012631	4.2007849	4.404	4.658	4.740	681.21	701.35	707.90	79.17
3S3-L	0.0054374	0.524238	4.643	4.886	4.965	950.30	994.86	1009.53	183.91
3T4	0.007018	2.2421119	4.642	4.885	4.965	980.99	1015.57	1026.88	142.49
3T6	0.0831947	61.91291	4.279	4.540	4.624	795.62	798.66	799.78	12.02

[1]: Units in kN.   Reference: Adapted from Moura (2019).

It was admitted that the coefficient of variation of the bending moment induced by each truck loading has the same values as the coefficient of variation of the respective truck weight (current or extrapolated). This assumption is reasonable since there exists a linear relation between the truck weights and the induced bending moment assuming that the distance between axles is deterministic. This assumption was also used by Ferreira et al. (2015). The coefficients of variation (V) are shown in Table 3.7, based on the means and standard deviations found in Table 3.6.

Table 3.7 - Coefficients of Variation (V) of the Gross Weights

Vehicle	$V_{15\ years}$	$V_{50\ years}$	$V_{75\ years}$
2S2	0.192	0.184	0.181
2S3-C	0.154	0.149	0.147
2S3-L	0.067	0.066	0.066
3S3-C	0.116	0.113	0.112
3S3-L	0.194	0.185	0.182
3T4	0.145	0.140	0.139
3T6	0.015	0.015	0.015

3.6 Structural Simulation

The structural simulations were carried out in CSIBridge software, which uses the Finite Element Method to discretize the structural system. The modeling is used to guarantee a monolithic discretized model (cast-in-place deck) that considers the stress variations along the cross sections of the structural elements, and for this, shell elements are used.

As boundary conditions were considered in the supports to simulate elastomeric support devices, properties of transversal elastic modulus (G) equivalent to 1.0MPa, thickness of 10

cm, and the cross section of 60x60 cm. In addition, one of the directions was considered fixed and the others were free.

The vehicles should be arranged longitudinally and transversally along the bridge deck to obtain the maximum bending moment. All analyses were subjected to the distributed load of 5 kN/m² since it is representative of the passing over of lighter vehicles and it is always considered to surround the vehicles, as provided by ABNT NBR 7188 (2013). In other words, the bending moments are obtained by replacing the Brazilian design vehicle with the chosen DNIT cataloged vehicles.
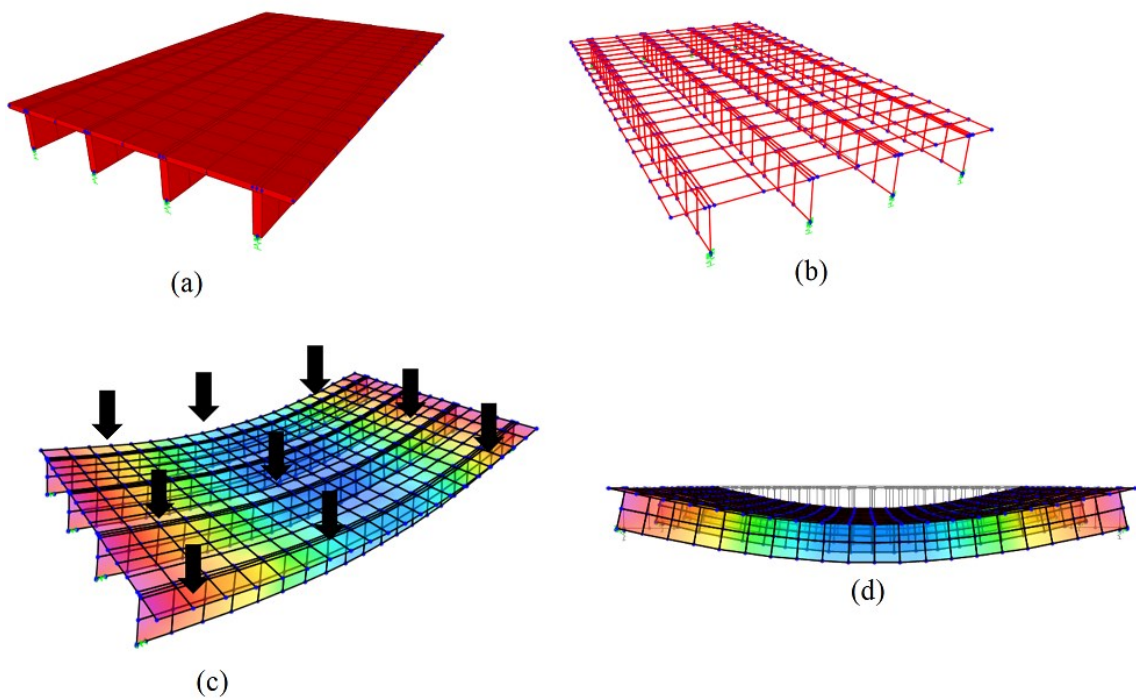

(a)

(b)

(c)

(d)

Figure 3.7 - Finite element model: (a) undeformed shape; (b) nodes and frames; (c) deformed shape due to loading; (d) deformed shape compared to undeformed shape.
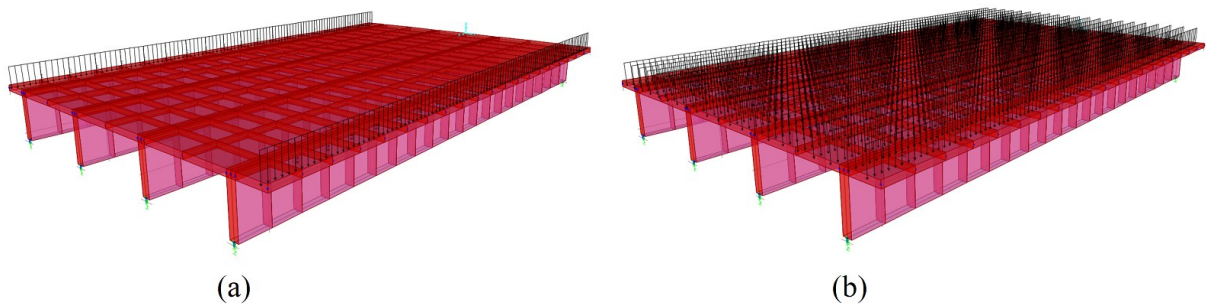

(a)

(b)

Figure 3.8 – Loading: (a) Guardrails; (b) Pavement.

In the case of the study considering the Brazilian standard was adopted a lane with a width equivalent to the sum of all traffic lanes for each section, followed by the application of two live loads. Configurations indicated the composition of two loads, one for the distributed load of 5 kN/m² and another for the TB-450 design vehicle or some chosen vehicles cataloged by DNIT with its occupation area, performing a linear sum between the results of the envelopes obtained for each of these loads. Regarding the distributed load, it must be applied in the CSIBridge software as a linear load per meter, i.e., in kN/m.
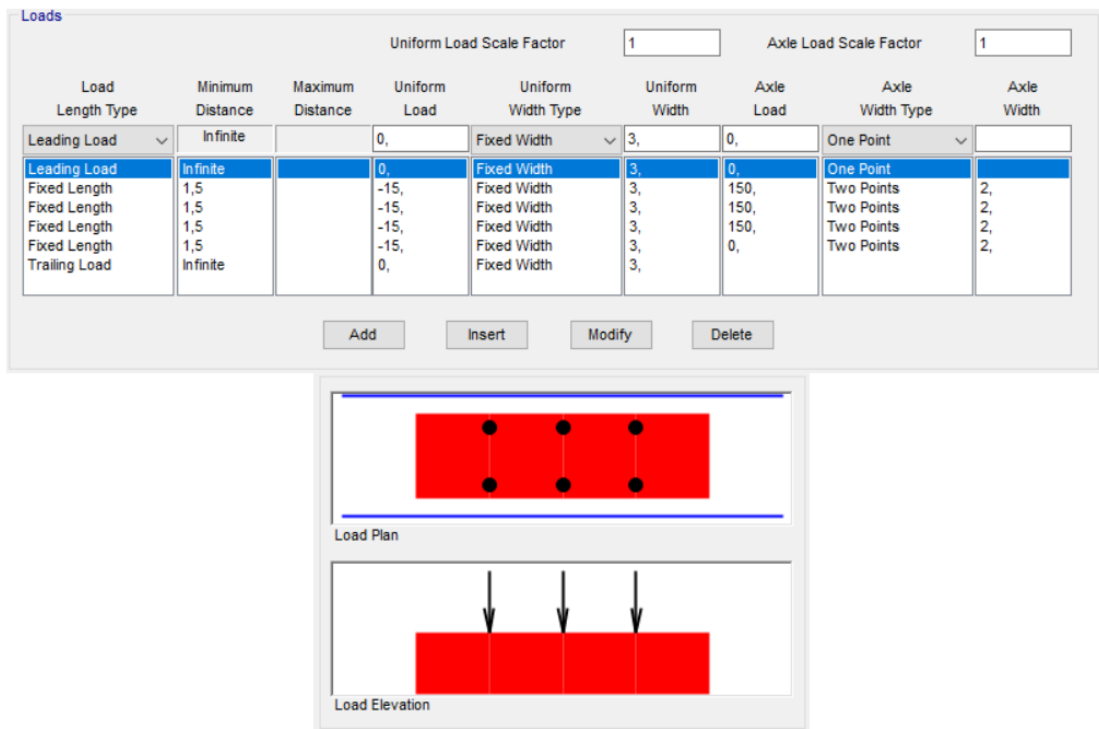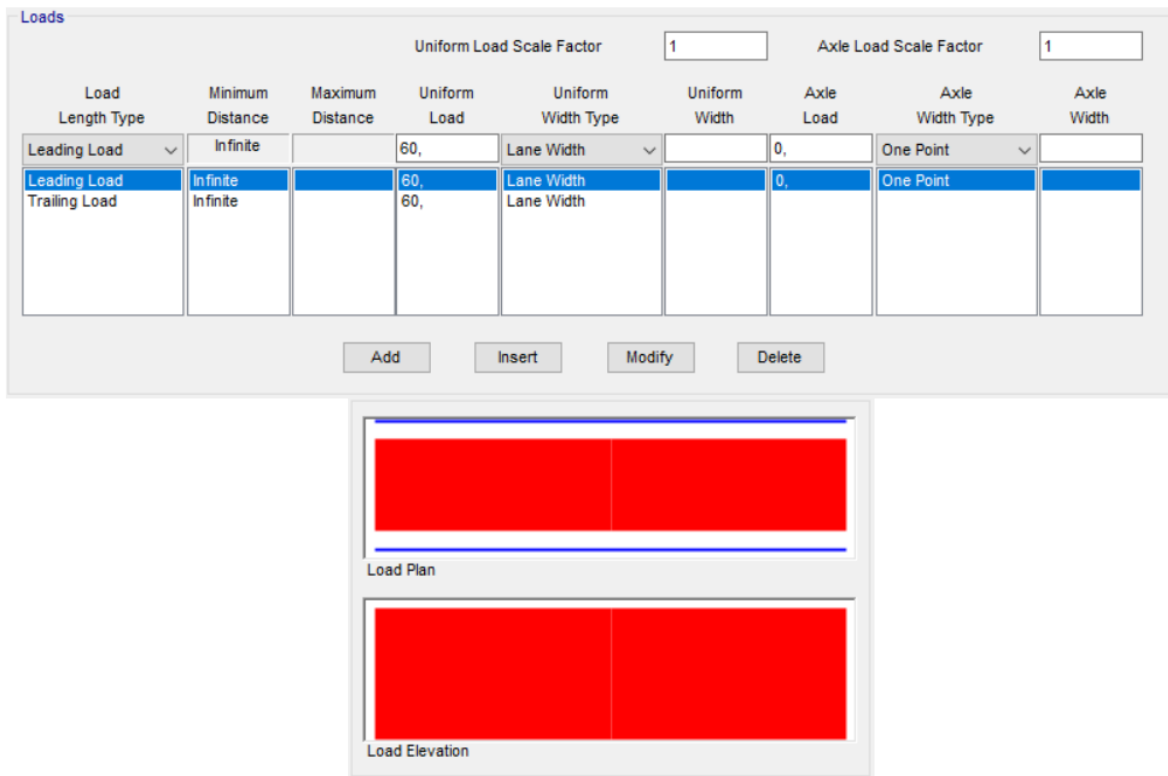

Figure 3.9 – TB-450 configuration.

Figure 3.10 – Distributed load configuration.

3.7 Loading Consideration

According to Ferreira et al. (2008), the maximum bending moments for bridges with short decks, such as those that were the subject of case studies in this dissertation, are generally obtained with the presence of one vehicle alone or two trucks side-by-side. Portela et al. (2017) surveyed the probabilities of simultaneous occurrences of heavy vehicles on bridges in Brazil, arriving at an average percentage of occurrence about total traffic of 0.079% for bridges studied in the state of São Paulo and 0.0186% for bridges in the state of Rio Grande do Sul. Thus, this work focused on the verification of isolated heavy trucks, given the higher probability of occurrence.

3.8 Monte Carlo Simulation for Uncertainty Quantification of Bending Moments

As expressed by Nowak (1999), Ferreira et al. (2008) and Portela (2018), the traffic load of each vehicle was assumed as a product of two parameters (LP), where L is the static live load effect and P is an analysis factor, whose mean is 1.00 and coefficient of variation V_P of 0.12. The LP coefficient of variation is given by:

$$V_{LP} = \sqrt{V_L^2 + V_P^2} \tag{11}$$

The coefficient of variation V_L refers to those designated in Table 3.3 and Table 3.7, depending on the return period to be studied. When including the portion referring to the dynamic effect, the statistical parameters of the maximum live load can be written as:

$$m_{LP+I} = 1.15 m_{LP} \tag{12}$$

$$\sigma_{LP+I} = \sqrt{\sigma_{LP}^2 + \sigma_I^2} \tag{13}$$

Which, $m_{LP}=m_L$ (bending moment obtained from the static live load), $\sigma_{LP}=V_{LP}m_{LP}$, $\sigma_I= V_I m_I$, and $m_I=0.15m_L$ with $V_I=0.80$. Regarding the actions referring to the dead load, for the cast-in-place structural elements (deck with slab and girders; guardrails) the probability distribution according to Santiago et al. (2020) was adopted and for the pavement, as there is no data for the probability distribution estimated in Brazil for this loading, the probability distribution parameters according to Nowak (1999) was adopted. The parameters bias factor ω (ratio between the mean and design value) and coefficient of variation V are shown in Table 3.8.

Table 3.8 - Statistical Parameters of the Dead Loads

Loads	ω	V	PDF
Self-weight of the structural elements and guardrails	1.06	0.12	Normal
Pavement	1.10	0.25	Normal

Source: Santiago et al. (2020) and Nowak (1999).

The analysis was done by generating 1 million values for each vehicle and each dead load, using Monte Carlo simulation, thus creating a model of possible results, using the respective probability distribution of each random variable.

Denominating the dead load of the structural elements as **dd1**, the guardrail load as **dd2**, the load referring to the pavement as **dd3,** and the traffic load with its respective dynamic effect as **ll**, it is possible to obtain the solicitation **s** as the sum of the portions of these loads. Assuming the generation of 1 million values as previously mentioned, it is possible to generate a vector with this number of elements, emphasizing that the vector referring to the traffic load should present values based on the relative frequencies of the vehicles studied. In other words, the vector **ll** is constituted by values of all the chosen vehicles, and the number of values to compose the vector for each of them is determined by their relative frequency as shown in Figure 3.4(b).

$$s = dd1 + dd2 + dd3 + ll \tag{14}$$

For the determination process of 1 million values for each random variable, in the first step uniformly distributed random numbers between 0 and 1 were generated, and subsequently, with the obtained values, they were transformed into others equivalent to the delimited probability distributions. Each random number generated, variable and uniform between 0 and 1, called u, can be interpreted as a value of cumulative probability to which should correspond to a cumulative distribution $F_X(x)$, according to Figure 3.11:
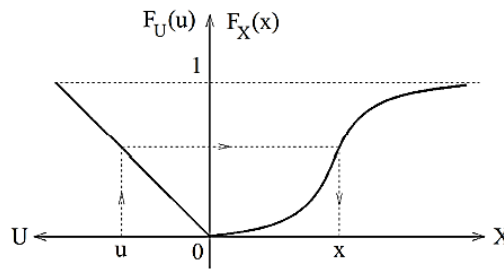

Figure 3.11 - Relation between u and x for random number generation. Source: Adapted from Ang and Tang (1984).

The equivalent value sought, corresponding to u, is the abscissa x. To obtain their respective value, the two cumulative distributions were equalized.

$$p[X \leq x] = p[U \leq u] \Rightarrow F_X(x) = F_U(u) \tag{15}$$

Since for the cumulative uniform distribution, $F_U(u) = u$, then:

$$F_X(x) = u \Rightarrow x = F_X^{-1}(u) \tag{16}$$

To obtain the number equivalent and corresponding to the random value of a known probability distribution according to the function $f_X(x)$, it is sufficient to take the inverse cumulative distribution of f_X. The Inverse Cumulative Density Functions (ICDF) are shown in Table 3.9, according to the location a, scale b and shape c parameters, from the mean μ and standard deviation σ, admitted in Table 3.10.

Table 3.9 - Inverse Cumulative Density Functions for Selected Probability Distributions

Distribution	ICDF
Normal	$a + b\Phi^{-1}(p)$
Gumbel	$a - bln[-\ln(p)]$
Double Exponential	$\begin{cases} a + b\ln(2p), \text{if } p < 0.5 \\ a - b\ln[2(1-p)], \text{if } p \geq 0.5 \end{cases}$
Minimum Extreme Value – Type II	$a - b[-\ln(1-p)]^{\frac{-1}{c}}$
Rayleigh	$a + b\sqrt{-2\ln(1-p)}$
Maximum Extreme Value – Type II	$a + b[-\ln(p)]^{\frac{-1}{c}}$

Table 3.10 - Mean and Standard Deviation in Terms of Parameters a, b, and c of Selected Probability Distributions

Distribution	μ	σ	Domain
Normal	a	b	$(-\infty, \infty)$
Gumbel	$a + \gamma b$	$\frac{\pi}{\sqrt{6}}b$	$(-\infty, \infty)$
Double Exponential	a	$b\sqrt{2}$	$(-\infty, \infty)$
Minimum Extreme Value – Type II	$a - b\Gamma(1-\frac{1}{c})$	$b\sqrt{\Gamma(1-\frac{2}{c}) - \Gamma^2(1-\frac{1}{c})}$	$(-\infty, a]$
Rayleigh	$a + b\sqrt{\frac{\pi}{2}}$	$b\sqrt{2-\frac{\pi}{2}}$	$[a, \infty)$
Maximum Extreme Value – Type II	$a + b\Gamma(1-\frac{1}{c})$	$b\sqrt{\Gamma(1-\frac{2}{c}) - \Gamma^2(1-\frac{1}{c})}$	$[a, \infty)$

For bimodal distributions, the probability density function can be expressed by the probability density functions that compose it:

$$f_X(x) = \varphi f_1(X) + (1 - \varphi)f_2(x) \tag{17}$$

Where φ is the mixing parameter, $f_1(x)$ is the first probability density function and $f_2(x)$ is the second probability density function.

Uniformly distributed random numbers u_1 and u_2 are then generated, such that the values to be found x, are obtained by taking the inverse cumulative distributions of $f_1(x)$ and $f_2(x)$, denoted by $F_1^{-1}(x)$ and $F_2^{-1}(x)$, respectively.

$$x = \begin{cases} F_1^{-1}(u_2), if \ u_1 < \varphi \\ F_2^{-1}(u_2), if \ u_1 \geq \varphi \end{cases} \tag{18}$$

CHAPTER 4 – RESULTS

In this chapter the results found will be presented in such a way that they are separated into two parts: one related to the uncertainty of the quantification of the bending moments, to show the histograms, and probability distributions that best fit and quantify values of the bending moments of the analyzed standards, and another section related to the structural reliability analysis, focused on the β index.

4.1 Uncertainty Quantification of Bending Moments

From the log-likelihood analysis, which can be adopted as a measure of fit, in which the smallest absolute value of this parameter is sought to select the best probability distribution that fits the proposed model, through the use of Matlab software, it was verified that the distribution that best applies to each histogram of the bending moments for the models studied was the Normal distribution for T=0, represented in Figure 4.1(a) and the Gamma distribution represented in Figure 4.1(b)-(d), for T=15 years, T=50 years and T=75 years, respectively, as a function of the bending moments obtained in the simulations (M_n) in kNm.
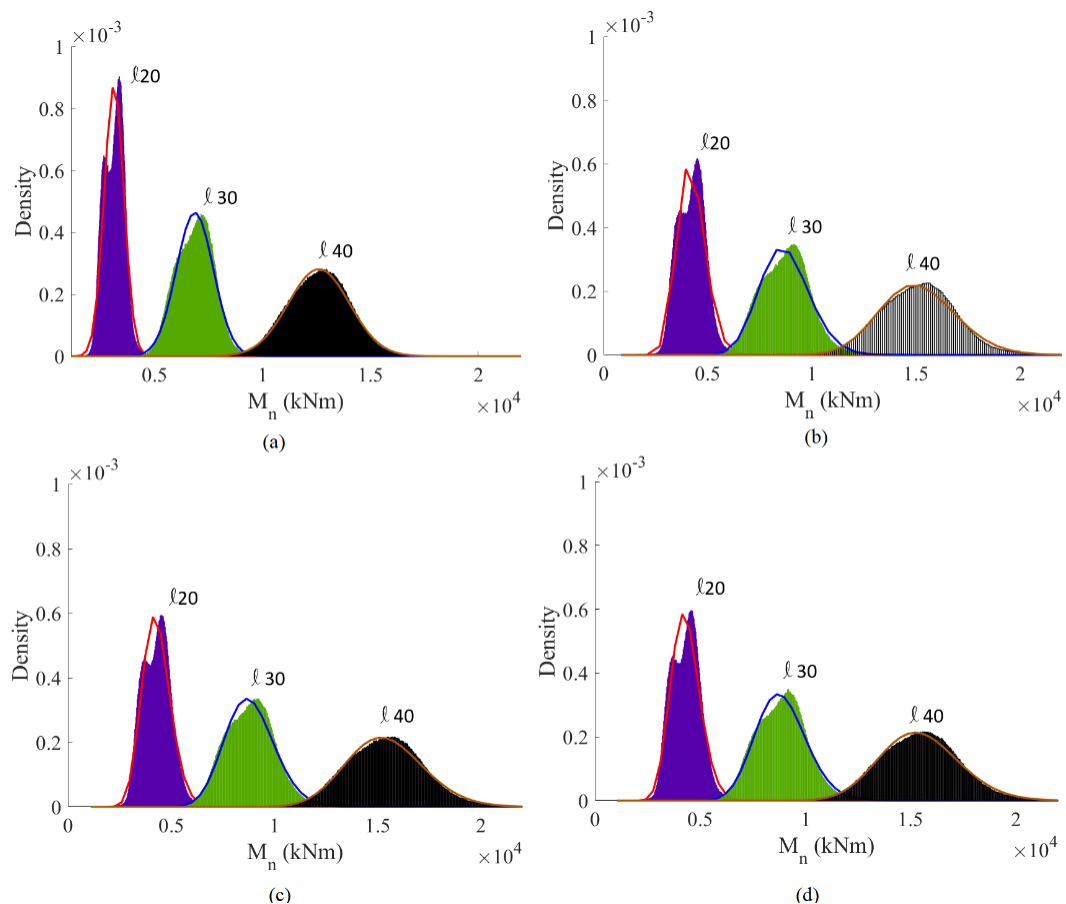

Figure 4.1 - Distribution fitting (a) T=0; (b) T=15 years; (c) T=50 years; (d) T=75 years.

For future events, the Gamma distribution is the best fit for bridges with characteristics like the studied ones. So, it can be used for estimated checks of the structural reliability parameters. The Gamma distribution can be described as a function of shape parameters k and scale θ, where $\Gamma(k)$ is the Gamma function evaluated at k and $\gamma(k, \frac{x}{\theta})$ is the incomplete Gamma function:

$$f(x) = \frac{1}{\Gamma(k)\theta^k} x^{k-1} e^{-\frac{x}{\theta}} \tag{19}$$

$$F(x) = \frac{1}{\Gamma(k)} \gamma(k, \frac{x}{\theta}) \tag{20}$$

The bending moments CDF referring only to traffic loads were plotted to verify the percentage of them exceeding the values of the TB-450 design vehicle. This is shown in Figure 4.2(a)-(c), where M_t means the bending moments related only to traffic loads. Also, the characteristic values for the Brazilian design vehicle (TB-450) are emphasized on each curve for the studied spans.
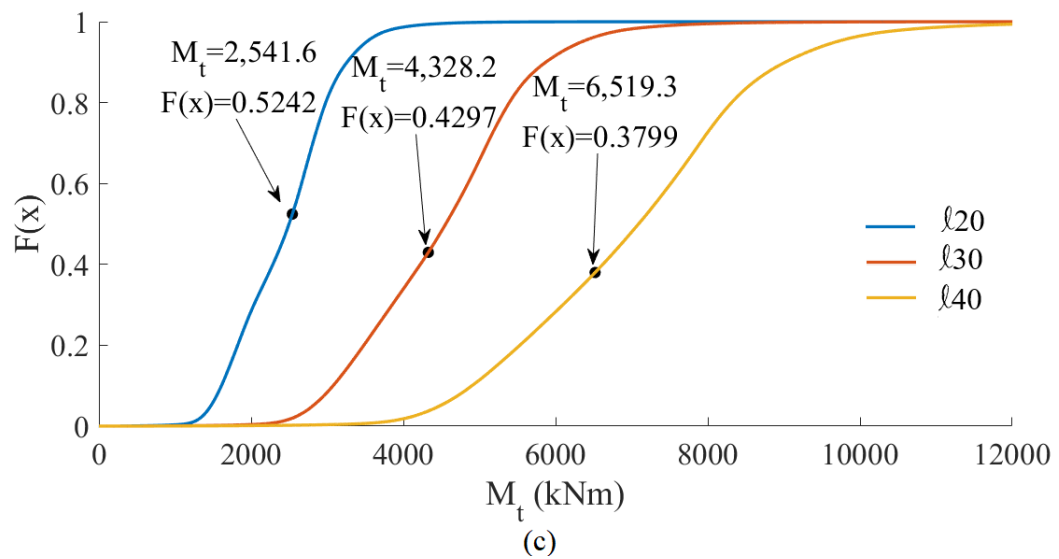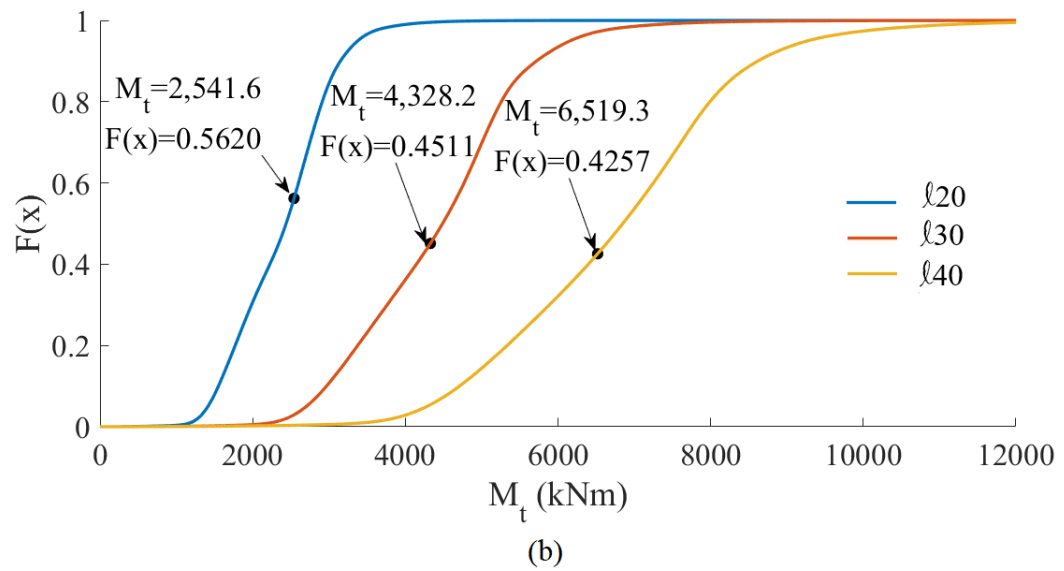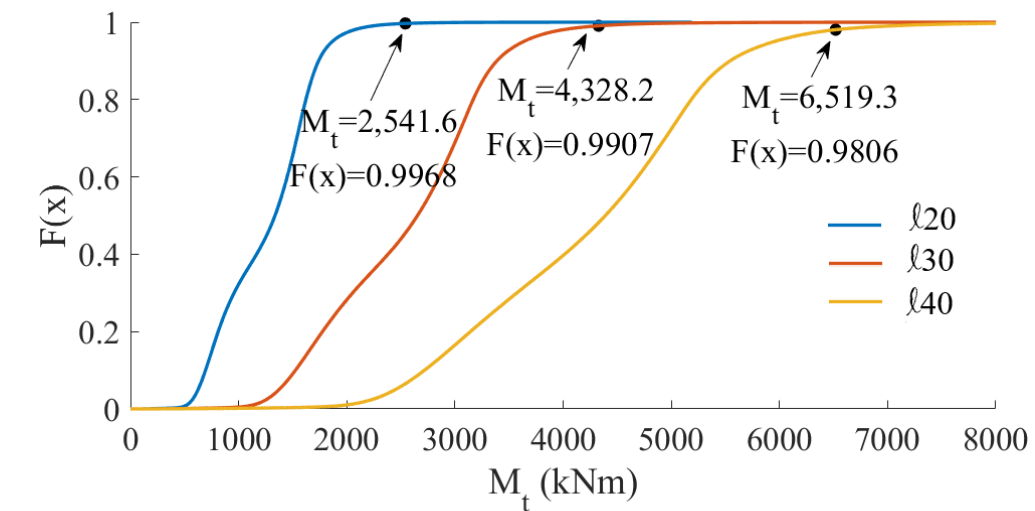
Figure 4.2 - Bending moments CDF related to the traffic loads for different ℓ: (a) T=0; (b) T=15 years; (c) T=50 years.

ABNT NBR 8681 (2003) claims that the characteristic values of live loads correspond to a percentage of 25% to 35% of being exceeded in the unfavorable direction during a period of 50 years, however, this situation is not configured and is evidenced in Figure 4.2(c), pointing out the characteristic value of TB-450, as 2,541.6 kNm, 4,328.2 kNm, and 6,519.3 kNm, respectively for model $\ell 20$, $\ell 30$, and $\ell 40$, in a return period of 50 years, all with its respective dynamic effect (impact load). The percentages exceeding the characteristic value in the unfavorable direction are 47.6% for $\ell 20$, 57.0% for $\ell 30$, and 62.0% for $\ell 40$.

As for the 15-year return period, it is observed that the values already exceed what the ABNT NBR 8681 (2003) recommends for what would be the 50-year return period, demonstrating that the actual loads of heavy vehicles demand more of the structures than the Brazilian design vehicle (TB-450). As shown in Figure 4.2(b), percentages exceeding the characteristic value in the unfavorable direction are 43.8% for $\ell 20$, 54.9% for $\ell 30$, and 57.4% for $\ell 40$.

The bending moment obtained from the structural analysis in the simulations of the model bridges (M_n) was presented in the form of histograms, in kNm, taking as reference for all cases the ultimate limit state for the Brazilian and American standards, in addition to characteristic values (without load factors). Using ABNT NBR 8681 (2003) and ABNT NBR 7188 (2013), it is evidenced the bending moments with load factors ($M_{NBR/F}$) and without load factors (M_{NBR}). Using AASHTO LRFD (2020), only the bending moment with their respective load factors ($M_{AASHTO/F}$) are shown. In addition, it is emphasized the mean of the bending moments (μ_M).
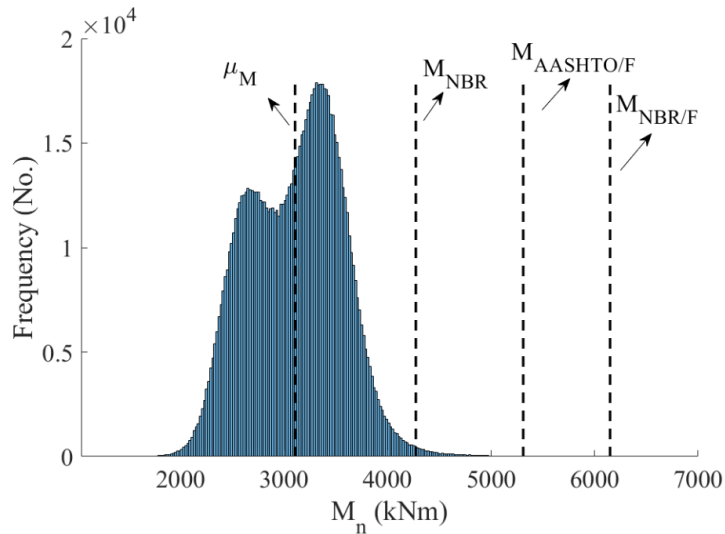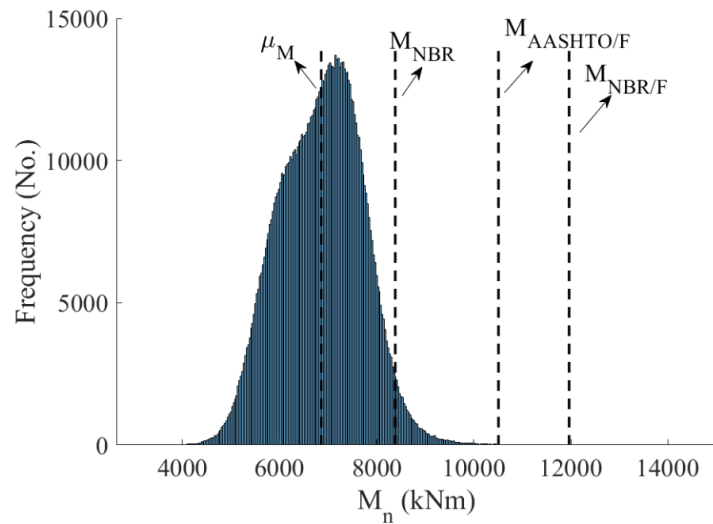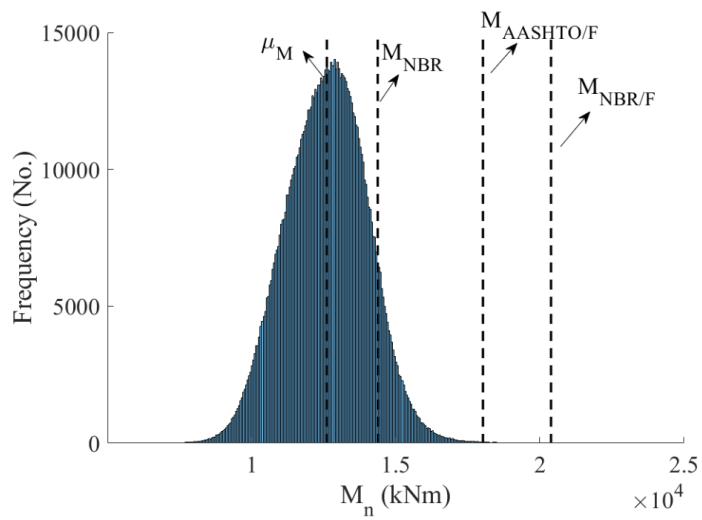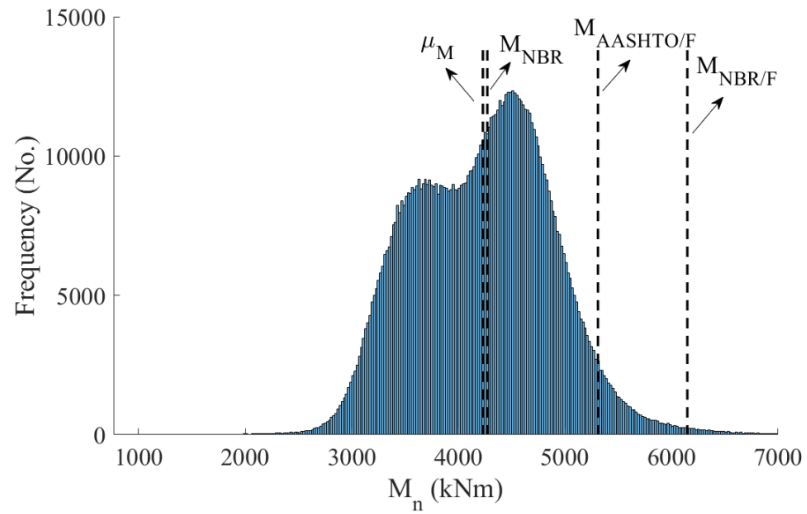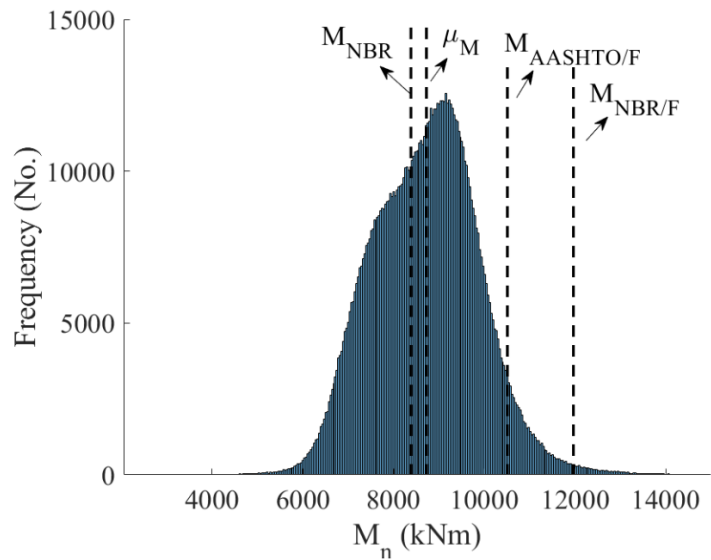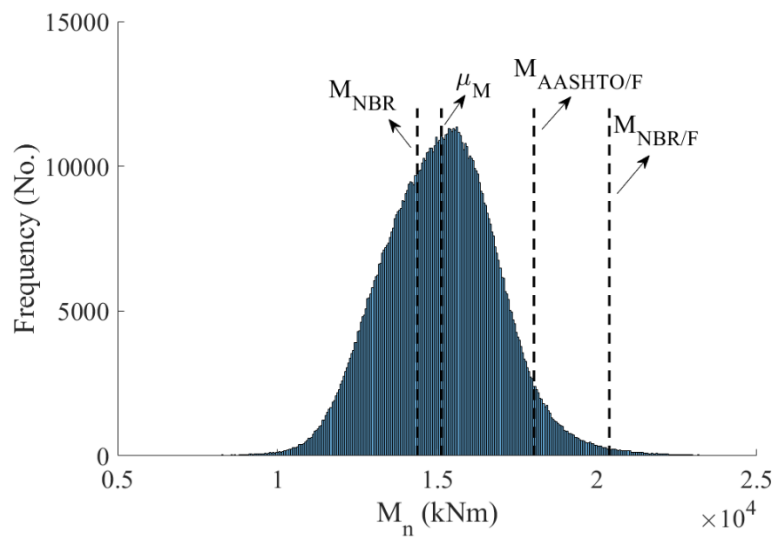
Figure 4.3 - Maximum bending moment histograms for T=0 (a) ℓ20; (b) ℓ30; (c) ℓ40.

(a)

(b)

(c)

48

Figure 4.4 - Maximum bending moment histograms for T=15 (a) $\ell 20$; (b) $\ell 30$; (c) $\ell 40$.

(a)

(b)
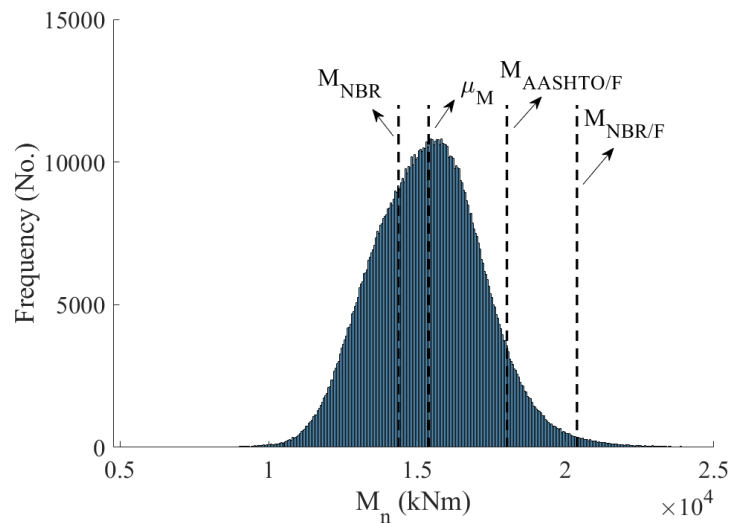
(c)

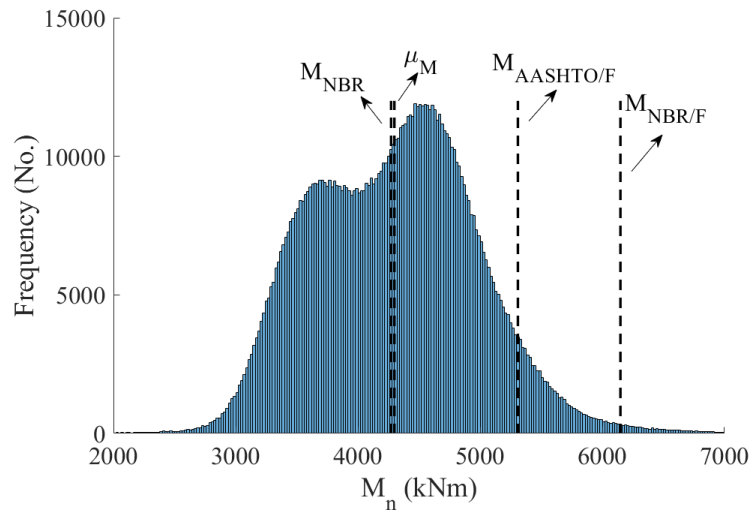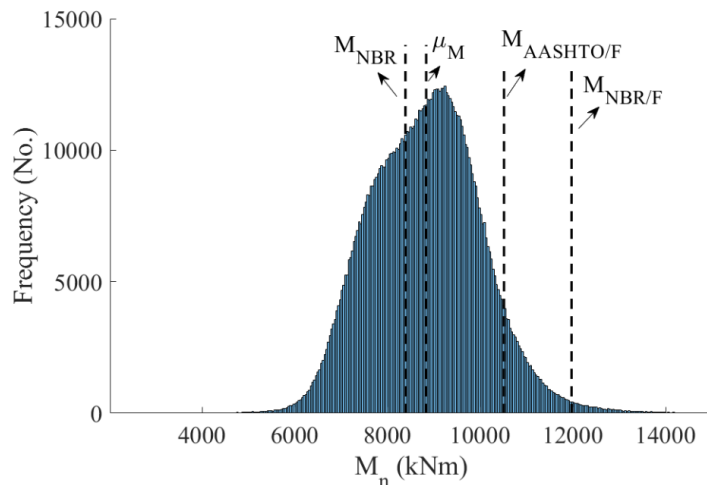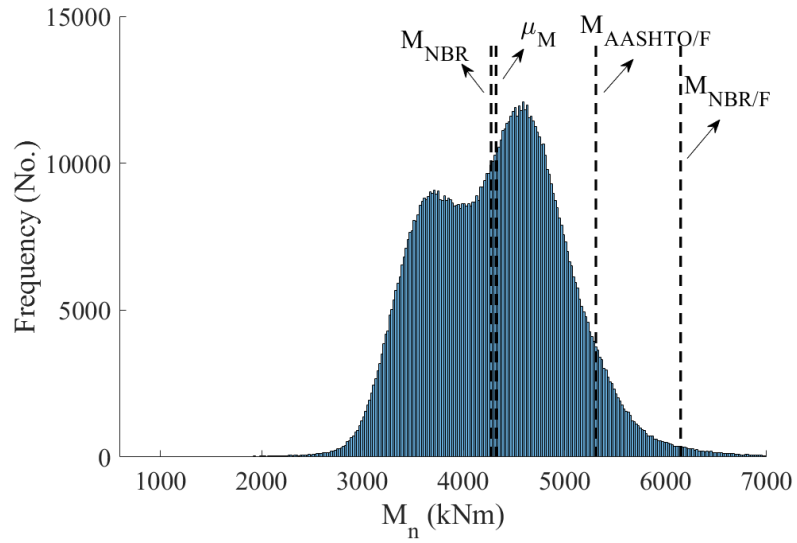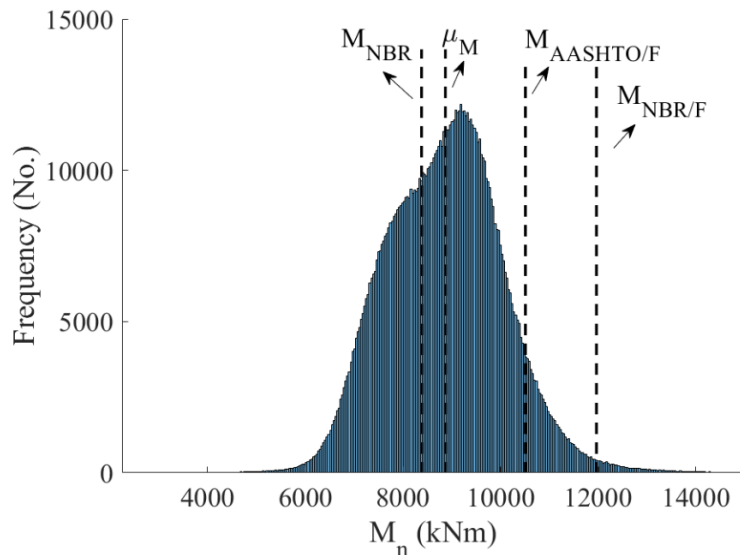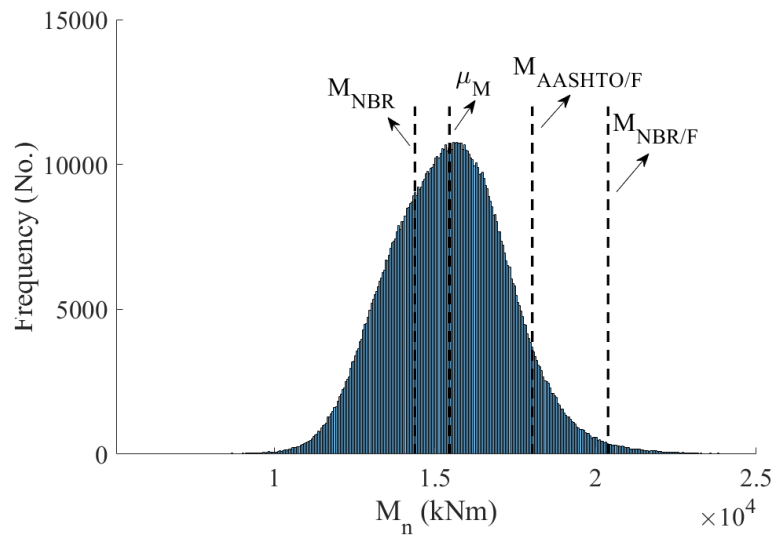Figure 4.5 - Maximum bending moment histograms for T=50 years (a) $\ell 20$; (b) $\ell 30$; (c) $\ell 40$.

Figure 4.6 - Maximum bending moment histograms for T=75 years (a) ℓ20; (b) ℓ30; (c) ℓ40.

The histograms obtained show that the bending moments found for the cases of extrapolated traffic were less conservative than those obtained for T=0, also noting little variability between the return periods of 50 and 75 years.

From the histograms (Figure 4.3 to Figure 4.6) it is possible to obtain ratios λ, obtained by Equation (21), and is shown in the Table 4.1 to Table 4.4, as a function of each analyzed time period.

$$\lambda_{NBR} = \frac{\mu_M}{M_{NBR}}$$

$$\lambda_{NBR/F} = \frac{\mu_M}{M_{NBR/F}}$$

$$\lambda_{AASHTO/F} = \frac{\mu_M}{M_{AASHTO/F}}$$

(21a,b,c)

Table 4.1 - Ratio λ Considering Traffic for T=0

λ	$\ell 20$	$\ell 30$	$\ell 40$
λ_{NBR}	$\frac{3104.9}{4272} = 0.73$	$\frac{6857.1}{8382} = 0.82$	$\frac{12612.7}{14377.1} = 0.88$
$\lambda_{NBR/F}$	$\frac{3104.9}{6148.4} = 0.50$	$\frac{6857.1}{11965} = 0.57$	$\frac{12612.7}{20387} = 0.62$
$\lambda_{AASHTO/F}$	$\frac{3104.9}{5309.6} = 0.58$	$\frac{6857.1}{10508.8} = 0.65$	$\frac{12612.7}{18027.2} = 0.70$

Table 4.2 - Ratio λ Considering Traffic for T=15 years

λ	$\ell 20$	$\ell 30$	$\ell 40$
λ_{NBR}	$\frac{4230.3}{4272} = 0.99$	$\frac{8724.6}{8382} = 1.04$	$\frac{15129.6}{14377.1} = 1.05$
$\lambda_{NBR/F}$	$\frac{4230.3}{6148.4} = 0.69$	$\frac{8724.6}{11965} = 0.73$	$\frac{15129.6}{20387} = 0.74$
$\lambda_{AASHTO/F}$	$\frac{4230.3}{5309.6} = 0.80$	$\frac{8724.6}{10508.8} = 0.83$	$\frac{15129.6}{18027.2} = 0.84$

Table 4.3 - Ratio λ Considering Traffic for T=50 years

λ	$\ell 20$	$\ell 30$	$\ell 40$
λ_{NBR}	$\frac{4298.6}{4272} = 1.00$	$\frac{8830.5}{8382} = 1.05$	$\frac{15391.6}{14377.1} = 1.07$
$\lambda_{NBR/F}$	$\frac{4298.6}{6148.4} = 0.70$	$\frac{8830.5}{11965} = 0.74$	$\frac{15391.6}{20387} = 0.75$
$\lambda_{AASHTO/F}$	$\frac{4298.6}{5309.6} = 0.81$	$\frac{8830.5}{10508.8} = 0.84$	$\frac{15391.6}{18027.2} = 0.85$

Table 4.4 - Ratio λ Considering Traffic for T=75 years

λ	ℓ20	ℓ30	ℓ40
λ_{NBR}	$\dfrac{4321.5}{4272} = 1.01$	$\dfrac{8869.4}{8382} = 1.06$	$\dfrac{15450.4}{14377.1} = 1.07$
$\lambda_{NBR/F}$	$\dfrac{4321.5}{6148.4} = 0.70$	$\dfrac{8869.4}{11965} = 0.74$	$\dfrac{15450.4}{20387} = 0.76$
$\lambda_{AASHTO/F}$	$\dfrac{4321.5}{5309.6} = 0.81$	$\dfrac{8869.4}{10508.8} = 0.84$	$\dfrac{15450.4}{18027.2} = 0.86$

The trend of the λ ratios shows how close the mean bending moments found are to the standard reference values (ultimate bending moments or bending moments without load factors). For λ values close to 1.00, there is a point where there is a 50% probability of failure of that structure, and the higher the λ value, the higher failure probability values are found.

Also, the histograms obtained and presented in Figure 4.3 to Figure 4.6, it is possible to obtain the bending moments (M_n), as a function of the quantity α of the respective CDF and compare them to the bending moments without load factors (M_k), obtained by ABNT NBR 7188 (2013) and AASHTO LRFD (2020), shown in Table 4.5.

Table 4.5 - Bending Moments M_k Obtained for the Models

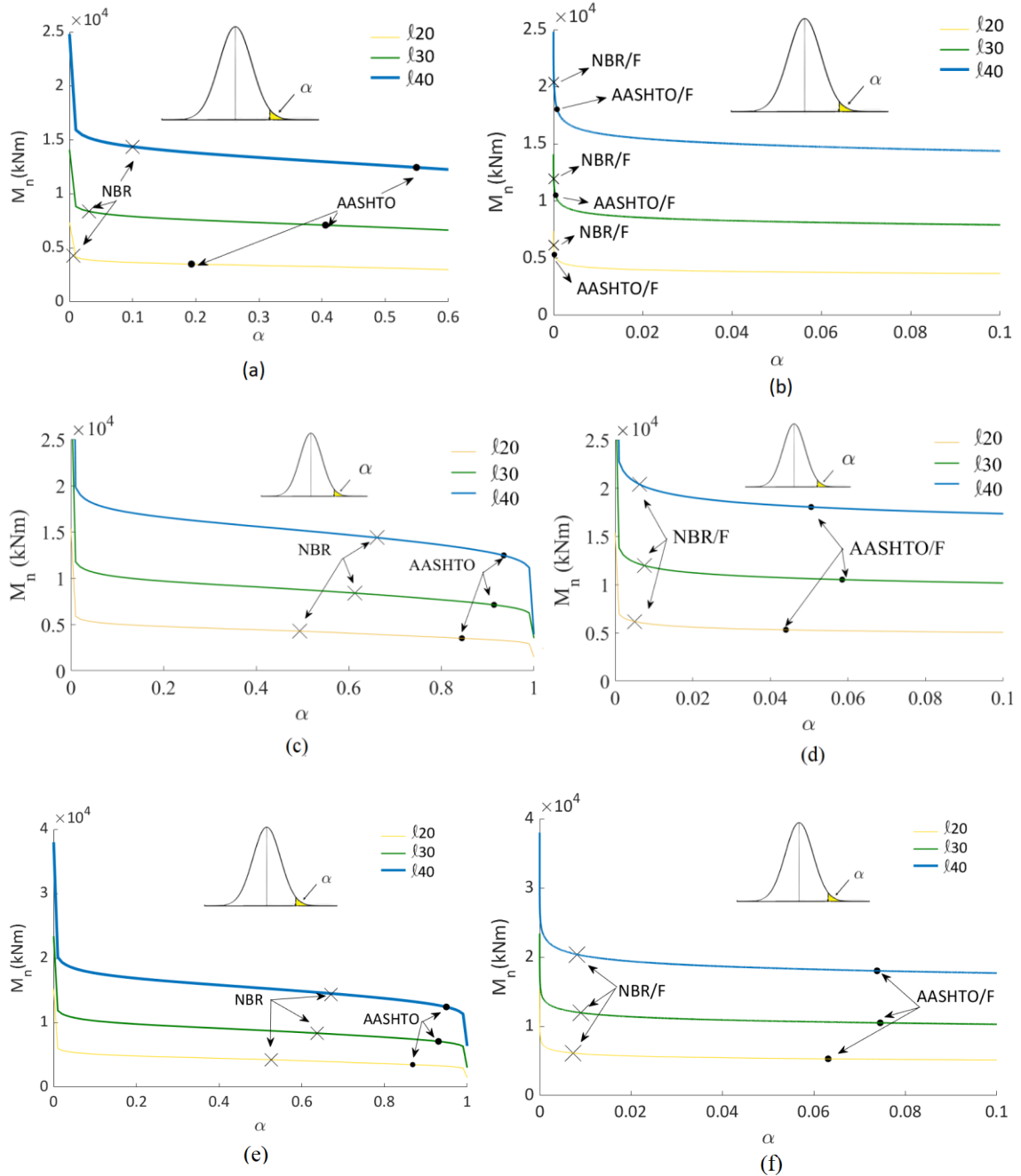| M_k (kNm)	ℓ20	ℓ30	ℓ40
NBR	4,272.0	8,382.0	14,377.1
AASHTO	3,506.7	7,112.3	12,453.4

Figure 4.7 - M_n as a function of α, emphasizing M_k (on graphs X and • values), (a) T=0; (c) T=15 years; (e) T=50 years, besides M_n emphasizing $\alpha \leq 0.1$, $M_{NBR/F}$ and $M_{AASHTO/F}$, (b) T=0; (d) T=15 years; (f) T=50 years.

It can be observed from Figure 4.7 that there is a tendency for the quantity α of the bending moments from NBR and AASHTO to increase, in general, as the span size and the analyzed return period increase. This aspect leads to a decrease in the structural reliability index of the model, whose values are shown in section 4.2. The quantity α obtained for each bending moment M_k obtained by the ABNT NBR 7188 (2013), called bellow as NBR, and AASHTO LRFD (2020), called bellow as AASHTO, according to the models and return period T analyzed, are shown in Figure 4.8:
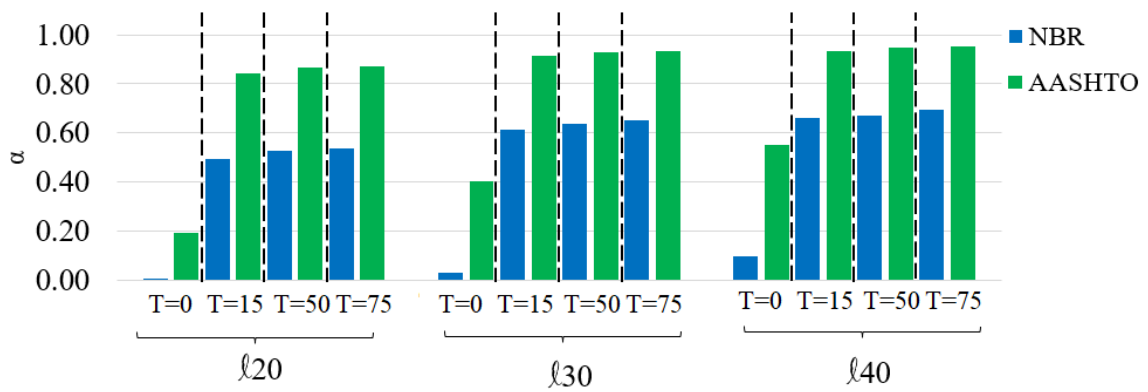
Figure 4.8 - Quantity α for each M_k for different T and ℓ.

For a return period of 50 years, it is possible to find a probability of approximately 65% of the M_k to be exceeded for model $\ell40$, following the assumptions of the ABNT NBR 7188 (2013), and approximately 95% to be exceeded for the same model and T, following the assumptions of the AASHTO LRFD (2020). In other words, what was obtained is that the mean values of the histograms are higher than the values found for bending moment without load factors, leading to values over 50% being exceeded in the unfavorable direction, which is a sign of attention regarding the safety of these structures.

4.2 Reliability Analysis

The reliability indexes were obtained according to Equation (8)-(9) and based on the histograms in Figure 4.3 to Figure 4.6 for the respective return periods, being distinguished for both the ABNT NBR 8681 (2003)/ABNT NBR 7188 (2013) and AASHTO LRDF (2020). Table 4.6 and Table 4.7 presents the reliability indexes for NBR (without load factors), NBR/F (with load factors), AASHTO (without load factors), and AASHTO/F (with load factors).

Also, it was decided to show what was found when taking as a resistance quantity reference, the bending moment of the standards without load factors, to observe which standard is more conservative when applying its respective load factors, from the variation obtained between the structural reliability indexes (Δβ).

Table 4.6 - Reliability Indexes of the Models Studied for American Standard

ℓ	AASHTO				AASHTO/F			
	$\beta_{T=0}$	$\beta_{15years}$	$\beta_{50years}$	$\beta_{75years}$	$\beta_{T=0}$	$\beta_{15years}$	$\beta_{50years}$	$\beta_{75years}$
20	0.86	(1.01)	(1.11)	(1.14)	3.51	1.71	1.53	1.50
30	0.24	(1.36)	(1.48)	(1.51)	3.30	1.57	1.44	1.42
40	(0.13)	(1.51)	(1.64)	(1.67)	3.15	1.64	1.46	1.41

Table 4.7 - Reliability Indexes of the Models Studied for Brazilian Standard

ℓ	NBR				NBR/F			
	$\beta_{T=0}$	$\beta_{15years}$	$\beta_{50years}$	$\beta_{75years}$	$\beta_{T=0}$	$\beta_{15years}$	$\beta_{50years}$	$\beta_{75years}$
20	2.51	0.02	(0.06)	(0.09)	4.13	2.56	2.44	2.41
30	1.87	(0.29)	(0.35)	(0.39)	3.90	2.43	2.36	2.34
40	1.28	(0.41)	(0.53)	(0.55)	3.69	2.50	2.42	2.37

The reliability indices in parentheses, in Table 4.6 and Table 4.7, show the cases in which the mean of the bending moment, for a particular case of span length and return period analyzed, is exceeding the reference bending moment value of that standard. These cases occur only for situations in which the load factors were not considered (M_{NBR} and M_{AASHTO}).

Regarding the conservatism between the Brazilian and American standards, it was noted that, in general, the American standard presents more conservatism when it refers to the application of their respective load factors since the $\Delta\beta$ found is higher than those for the Brazilian standard, i.e., the probability of failure decreases more when applying the load factors in the case of the American standard. This is evidenced in Table 4.8.

Table 4.8 – $\Delta\beta$ for the American and Brazilian Standards

ℓ	AASHTO LRFD (2020)				ABNT NBR 8681 (2003)/ABNT NBR 7188 (2013)			
	$\beta_{T=0}$	$\beta_{15years}$	$\beta_{50years}$	$\beta_{75years}$	$\beta_{T=0}$	$\beta_{15years}$	$\beta_{50years}$	$\beta_{75years}$
20	2.65	2.72	2.64	2.64	1.62	2.54	2.5	2.5
30	3.06	2.93	2.92	2.93	2.03	2.72	2.71	2.73
40	3.28	3.15	3.1	3.08	2.41	2.91	2.95	2.92

Commonly, international codes recommend target values for reliability indexes β_T, i.e., the structure should present a reliability index greater than or equal to these values $\beta \geq \beta_T$.

Taking some of these codes as a reference can be cited the *fib* Model Code for Concrete Structures (2010) and Probabilistic Model Code - PMC (2001), which delimit target reliability indexes for the ultimate limit state considering both the relative cost of increasing safety and the degree of failure consequence. Assuming that for typical bridges, the degree of failure consequence is moderate, i.e., if the ultimate limit state is reached for this type of structure, the damage with human and economic losses, besides social and environmental damages is considered moderate and that the relative costs of increasing safety are also moderate, the following values can be taken as a basis for the structural reliability indexes for the periods of 1 year, 15, 50 and 75 years, as shown in Table 4.9. Some reliability indexes were obtained from a known reliability index for a given reference period of n time units, as a function of that relative to 1 year, β_1, such as $\Phi(\beta_n) = [\Phi(\beta_1)]^n$.

Table 4.9 - Target Reliability Index Adopted by *fib* (2010) and PMC (2001)

Source	β_T			
	1 year	15 years	50 years	75 years
fib (2010)	4.70	4.10	3.80	3.70
PMC (2001)	4.20	3.50	3.20	3.10

Also, it can be cited the target reliability index adopted by the AASHTO LRFD (2020) was 3.5 for conventional and typical design bridges, whose return period is 75 years. From these international sources, it is observed that all the reliability indexes obtained, in Table 4.6 and Table 4.7, are lower than the β_T for return periods of 15, 50, or 75 years. For the current traffic (T=0), it can also be said that this presents lower reliability indexes than target indexes if compared to the reference period of 1 year.

The fact that the reliability indexes found were lower than those recommended by international model codes, characterizes the use of actual heavy vehicles showing lower reliability of the bridges than the one for which the structure was designed.
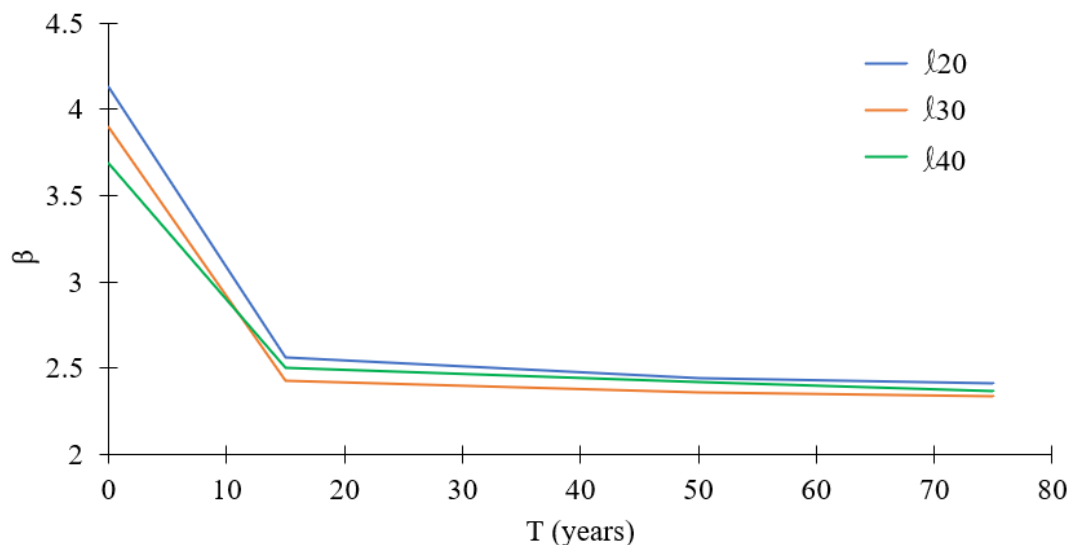

Figure 4.9 - Structural reliability indexes over the years for $M_{NBR/F}$.

From the results, over time the reliability indexes decrease but tend to converge to a single value independent of the model. This is because the bending moments tend to increase insignificantly after 50 years in the extrapolation process. Nowak (1999) found differences between bending moments for 50 and 75 years to be only about 1%. It is also observed that the reliability indexes are lower when using the AASHTO LRFD (2020) as a parameter if compared to the ABNT NBR 7188 (2003) and ABNT NBR 8681 (2013).

In general, the reliability index tends to decrease as the span length increases. However, it was observed that the ℓ30 started to present, throughout the return period, slightly lower reliability indexes in comparison to the ℓ40, which can be justified by the character of the vehicles used (length and axle spacing) when considered with their respective extrapolated weights.

Generalizing for these cases with bridge configurations equivalent to those studied, the value of the failure probability p_f and reliability index β can be estimated as a function of a ratio λ, according to Equation (21a,b,c).

To obtain the relation of λ with β and p_f, it is considered that the coefficient of variation remains constant, the shape and scale parameters for the Gamma distribution (best fit found for future events) are obtained as a function of the means μ and standard deviations σ found for each histogram of the studied bridges, and the respective probability of failure found are shown below.

$$\mu = k\theta \tag{22}$$

$$\sigma^2 = k\theta^2 \tag{23}$$

$$p_f = P(M_n > M_{NBR})$$

$$p_f = P(M_n > M_{NBR/F}) \tag{24a,b,c}$$

$$p_f = P(M_n > M_{AASHTO/F})$$

In this context, Figure 4.10 and Figure 4.11 shows the relation of λ with β and p_f, respectively, evidencing the values already found for the reliability indexes (Table 4.6 and Table 4.7) from the parameters of the histograms for the extrapolated traffic with T=15 years and T=50 years, considering ABNT NBR 8681 (2003), ABNT NBR 7188 (2013) and AASHTO LRFD (2020).
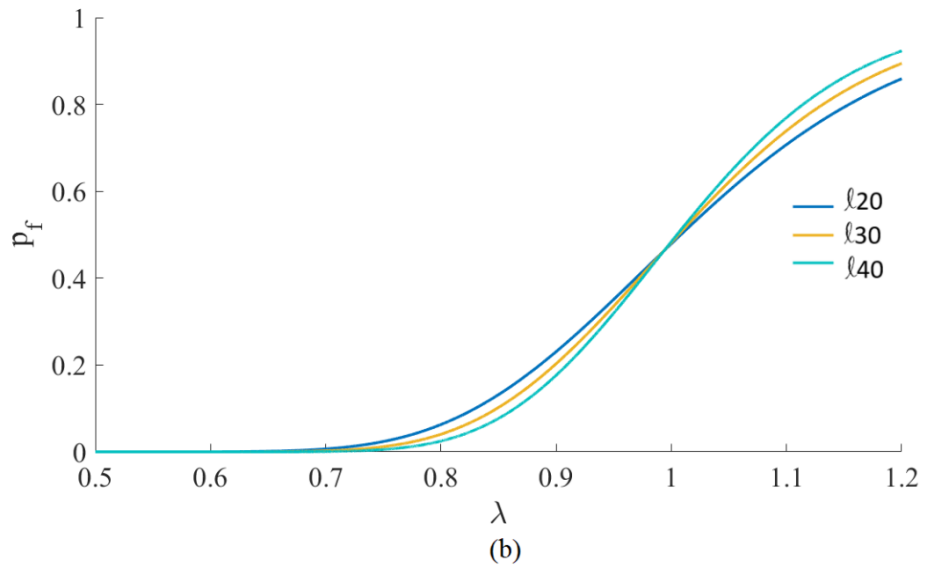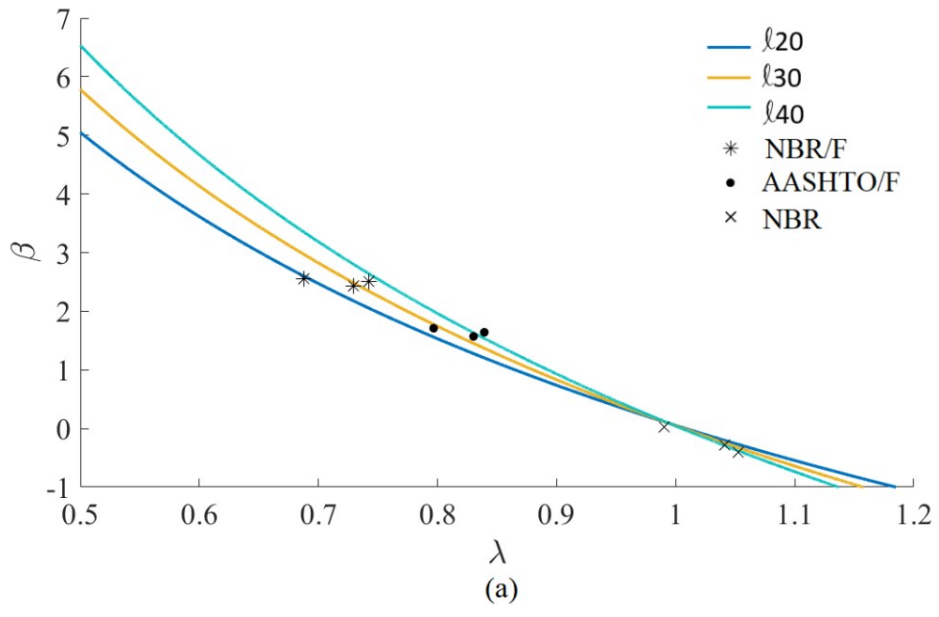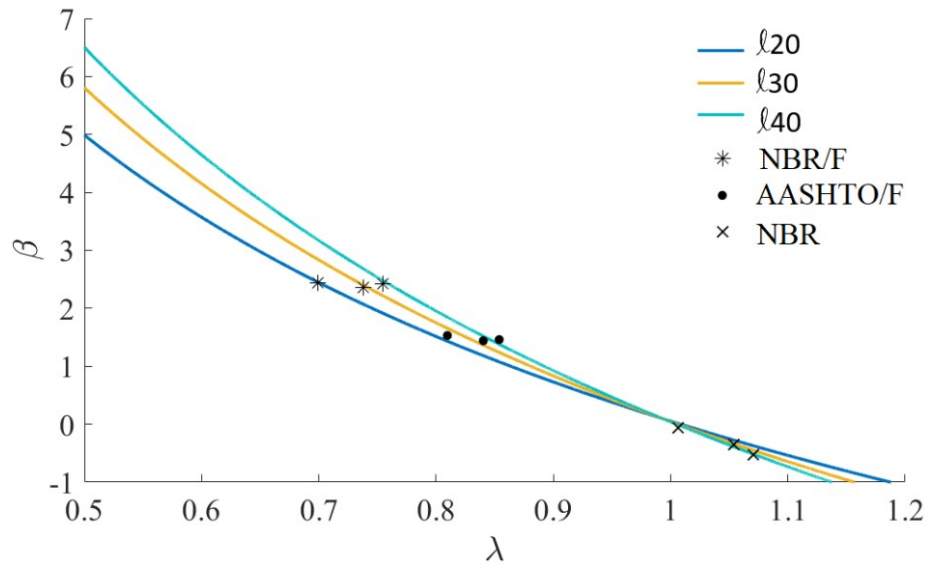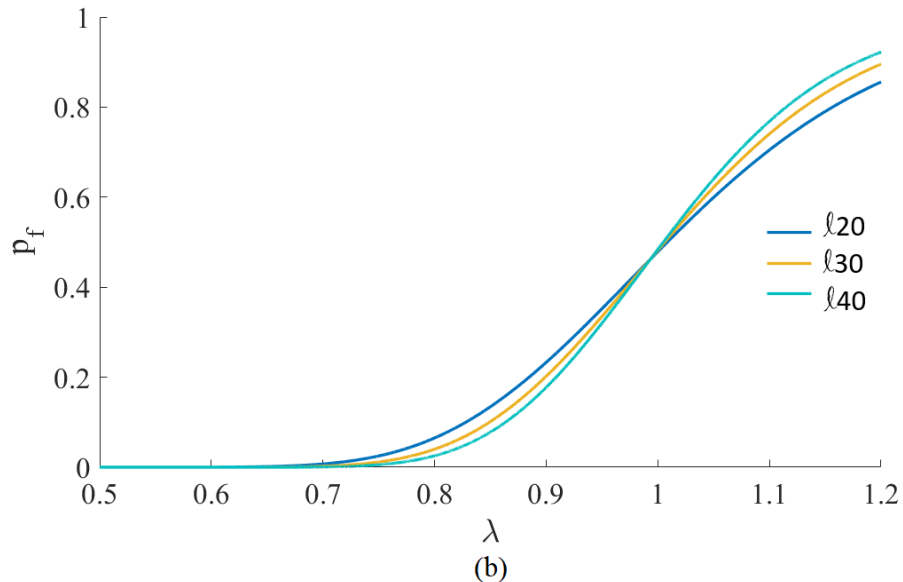
Figure 4.10 - Ratio λ for T=15 years in function (a) β; (b) p_f.

Figure 4.11 - Ratio λ for T=50 years in function (a) β; (b) p_f.

It is observed that when the mean of the bending moment is close to the reference value (M_{NBR}, $M_{NBR/F}$, or $M_{AASHTO/F}$), that is λ equal to 1.00, the respective failure probabilities are close to 50% (β=0), being this a point of change of behavior among the spans. When $\lambda<1.00$, for the same λ the probability of failure is higher for smaller spans, while $\lambda>1.00$, for the same λ the probability of failure is higher for larger spans.

As mentioned in section 3.2, the study performed has a basic hypothesis that the bridges do not present pathologies that could compromise their structural integrity. However, if a loss of load-carrying capacity is observed, the reliability indexes are reduced. To exemplify this reduction, the percentages of 2.5%, 5.0%, and 7.5% of loss of load carrying as a function of the

ULS pre-established, being T=0, T=15, and T=50 years taken as a hypothesis, to emphasize the requirement for constant maintenance of bridges.

In other words, percentages of 97.5%, 95%, and 92.5% of the ultimate bending moments of the Brazilian standard ($M_{NBR/F}$) and American standard ($M_{AASHTO/F}$) were adopted as resistance quantity R. The reliability indexes are shown in Table 4.10 to Table 4.12.

Table 4.10 - Reliability Indexes Considering ULS Loss Percentages for T=0

Model	NBR/F			AASHTO/F		
	2.5%	5.0%	7.5%	2.5%	5.0%	7.5%
ℓ20	4.08	3.90	3.81	3.40	3.29	3.18
ℓ30	3.75	3.66	3.54	3.19	3.07	2.93
ℓ40	3.57	3.46	3.36	3.01	2.86	2.69

Table 4.11 - Reliability Indexes Considering ULS Loss Percentages for T=15 years

Model	NBR/F			AASHTO/F		
	2.5%	5.0%	7.5%	2.5%	5.0%	7.5%
ℓ20	2.43	2.30	2.16	1.51	1.30	1.08
ℓ30	2.29	2.14	1.96	1.36	1.13	0.89
ℓ40	2.35	2.18	2.00	1.41	1.16	0.90

Table 4.12 - Reliability Indexes Considering ULS Loss Percentages for T=50 years

Model	NBR/F			AASHTO/F		
	2.5%	5.0%	7.5%	2.5%	5.0%	7.5%
ℓ20	2.32	2.18	2.02	1.34	1.15	0.94
ℓ30	2.21	2.04	1.85	1.23	1.01	0.77
ℓ40	2.25	2.07	1.86	1.22	0.97	0.72

Table 4.13 - Reliability Indexes Considering ULS Loss Percentages for T=75 years

Model	NBR/F			AASHTO/F		
	2.5%	5.0%	7.5%	2.5%	5.0%	7.5%
ℓ20	2.29	2.15	1.99	1.30	1.10	0.89
ℓ30	2.19	2.02	1.82	1.20	0.98	0.74
ℓ40	2.20	2.02	1.81	1.18	0.93	0.68

As expected, the structural reliability indexes obtained, considering losses of resistant capacity in function of the pre-established design for ULS, were lower, which generates the need for constant monitoring of the maintenance of these types of structures to avoid pathologies that can compromise the structural efficiency with the increase of the probability of failure p_f.

CHAPTER 5 – CONCLUSIONS

The dissertation presented a method to evaluate forces in comparison with a designated design vehicle, taking as a case study the ultimate bending moment generated by Brazilian design vehicle (TB-450), given by ABNT NBR 7188 (2013), and American design vehicle given by AASHTO LRFD (2020). The analysis was performed by comparing with real and extrapolated traffic of chosen DNIT cataloged vehicles, which are those most frequent in the observations and among those heavier (2S2, 2S3-C, 2S3-L, 3S3-C, 3S3-L, 3T4, and 3T6), according to the database adopted.

Three concrete bridge models were evaluated from Monte Carlo simulations, seeking to understand how adequate the design traffic loads contrast with the inherent uncertainties, from the standpoint of structural reliability, for the return period of 15, 50, and 75 years, in addition to T=0.

It was verified, in general, that the structural reliability indexes found, for all the return periods analyzed, are lower than the target values stipulated by international codes, such as *fib* Model Code for Concrete Structures (2010), Probabilistic Model Code - PMC (2001) and AASHTO LRFD (2020), thus pointing out an opportunity to improve ABNT NBR 8681 (2003) and ABNT NBR 7188 (2013) about traffic loads and bridges. These lower β_T values show that the actual traffic load that is currently passing over the highways results in lower reliability of the bridges, which may bring the opportunity to perform some calibration effects of the current Brazilian standards to reach the target values of the reliability indexes.

It is important to emphasize that this concern with structural safety is even more relevant for bridges, whose design process used older design parameters and whose design vehicle was even more conservative, which can be concluded that these structures have even lower structural reliability indexes compared to those found in this work.

Regarding only the traffic loads, a higher percentage of the characteristic values of the live loads are exceeded in the unfavorable direction than that recommended by ABNT NBR 8681 (2003). It was verified a percentage of approximately 47.6% of the characteristic values of the live loads to be exceeded in the unfavorable direction for model $\ell 20$ and a return period of 50 years, in contrast to the values of 25% to 35% recommended by the ABNT NBR 8681 (2003).

From the histograms found from the probability distributions for each type of vehicle studied, it was observed that the Gamma distribution had the lowest absolute value of the log-

likelihood parameter for the return periods of 15, 50, and 75 years, and this distribution was adopted to obtain any reliability index as a function of the ratio λ.

An aspect obtained from this study was that very long return periods end up producing little variability in the results, such as a difference of only about 1% compared to the return periods of 50 and 75 years. Furthermore, it can be said that very long return periods are not representative, given the constant change in traffic, either because of the technological advancement of vehicles or the characteristics of the products transported.

Another problem that can be raised is the use of foreign standards for local design, such as the AASHTO LRFD (2020) for the design of bridges considering the Brazilian real traffic. It is noted that the characteristic values of bending moment, when using American design vehicle, were lower compared to those obtained by the Brazilian one, being even more serious when the traffic was analyzed with the extrapolation of the gross weights of vehicles. Therefore, this aspect leads to lower reliability indexes than those using the ABNT NBR 8681 (2003) and ABNT NBR 7188 (2013) as the design assumption.

Finally, it is important to emphasize that the constant verification of traffic loads in bridges should be periodically performed to understand its evolution. No less important, it is necessary to constantly monitor the highways through the weighing of vehicles so that they can subsidize works like this one, in addition to ensuring the structural safety of bridges, since as verified, structures like that with pathological conditions have their structural reliability indexes decreased.

5.1 Future Works

The present study presented a method to analyze the standard design criteria for bridges, to verify the suitability of these parameters when compared to real traffic on these structures.

It is understood that within the method presented, some aspects can be refined to further improve what was proposed. In this way, it is recommended for future works:

i. Obtaining reliability indexes for fatigue and service limit states can be calculated;

ii. Inclusion of more bridge geometries, including variations in the number of girders and for larger spans/lengths so that the simultaneous presence analysis is relevant;

iii. Inclusion of the dynamic effect for cases developed especially for Brazilian bridges; and

iv.Inclusion of the uncertainty of axis spacing.

REFERENCES

AASHTO. (2020). AASHTO LRFD Bridge Design Specifications. American Association of State Highway and Transportation Officials, 9th Edition, Washington, DC.

ABCR. (2022). Brazilian association of highway concessionaires, available in <https://melhoresrodovias.org.br/>.

ABNT. (2003). NBR 8681: Actions and safety of structures - Procedure. Brazilian Association of Technical Standards, 1st Edition, Rio de Janeiro.

ABNT. (2013). NBR 7188: Road and pedestrian live load on bridges, viaducts, footbridges, and other structures. Brazilian Association of Technical Standards, 2nd Edition, Rio de Janeiro.

ABNT. (2014). NBR 6118: Design of concrete structures - Procedure. Brazilian Association of Technical Standards, 3rd Edition, Rio de Janeiro.

ABNT. (2020). NBR 7187: Design of concrete bridges, viaducts and footbridges. Brazilian Association of Technical Standards, 2nd Edition, Rio de Janeiro.

Alampalli, S., Frangopol, D.M., Grimson, J., Halling, M.W., Kosnik, D.E., Lantsoght, E.O.L., Yang, D., Zhou, Y.E. (2021). Bridge Load Testing: State-of-the-Practice. Journal of Bridge Engineering, 26(3), 03120002, doi:10.1061/(asce)be.1943-5592.0001678.

Ang, A. H.-S, Tang, W.H. (1984). Probability Concepts in Engineering Planning and Design. Volume II: Decision, Risk, and Reliability. New York, USA, John Wiley & Sons.

Bosso, M., Vasconcelos, K.L., Lee Ho, L., Bernucci, L.L.B. (2019). Use of regression trees to predict overweight trucks from historical weigh-in-motion data. Journal of Traffic and Transportation Engineering (English Edition), doi: 10.1016/j.jtte.2018.07.004.

Braz, D.H.L. (2019). Avaliação das normas correntes diante das incertezas dos parâmetros de projeto: estudo da norma de pontes de concreto armado, Dissertação de Mestrado, Departamento de Engenharia Civil e Ambiental, Universidade de Brasília.

Caprani, C.C., O'Brien, E.J., Lipari, A. (2016). Long-span bridge traffic loading based on multi-lane traffic micro-simulation. Engineering Structures, Vol. 115, pp. 207-219, doi: 10.1016/j.engstruct.2016.01. 045.

CONTRAN. (2006). Resolution No. 210/2006. National Transit Council, Brasilia, Brazil.

DNIT. (2012). Quadro de Fabricantes de Veículos. National Department of Transportation Infrastructure, Highway Infrastructure Board, General Coordination of Highway Operations, Rio de Janeiro.

El Debs, M.K., Malite, M., Takeya, T., Munaiar Neto, J., Hanai, J. B., Oliveira, P. E. (2005). Análise das consequências do tráfego de combinações de veículos de carga (CVCs) sobre as pontes da rede viária sob a jurisdição do DER-SP. Revista Minerva, São Carlos, v. 1, n.1, p. 27-35.

Ferreira, L.M., Nowak, A.S., El Debs, M.K. (2008). Development of truck weight limits for concrete bridges using reliability theory. Ibracon Structures and Materials Journal, 1(4), 421-450, doi:10.1590/s1983-41952008000400005.

fib Model Code for Concrete Structures. (2010). International Federation for Structural Concrete. *fib* Journal Structural Concrete, Lausanne.

Ghosn, M., Frangopol, D.M., McAllister, T.P., Shah, M., Diniz, S.M.C., Ellingwood, B.R., Manuel, L., Biondini, F., Catbas, N., Strauss, A., Zhao, X. L. (2016). Reliability-Based Performance Indicators for Structural Members. Journal of Structural Engineering, 142(9), F4016002, doi:10.1061/(asce)st.1943-541x.000154.

Gonçalves, M.S., Holdorf Lopez, R., Valente, A.M. (2022). Model Updating Using Hierarchical Bayesian Strategy Employing B-WIM Calibration Data. Journal of Bridge Engineering, v. 27, p. 04022023-1, 2022.

Hwang, E-S., Koh, H.M. (2000). Simulation of bridge live load effect. In: 16th Congress of IABSE, 2000.

Jacinto, L.A.C., Neves, L.A.C., Santos, L.M.P.O. (2015). Bayesian assessment of an existing bridge: a case study. Structure and Infrastructure Engineering, 12(1), 61–77, doi:10.1080/15732479.2014.995105.

Kala, Z. (2019). Global sensitivity analysis of reliability of structural bridge system. Engineering Structures, 194, 36–45, doi:10.1016/j.engstruct.2019.05.045.

Khan, M.S., Caprani, C., Ghosh, S., Ghosh, J. (2021). Value of strain-based structural health monitoring as decision support for heavy load access to bridges. Structure and Infrastructure Engineering, 1–16. doi:10.1080/15732479.2021.1890140.

Lu, N., Beer, M., Noori, M., Liu, Y. (2017). Lifetime deflections of long-span bridges under dynamic and growing traffic loads. Journal of Bridge Engineering, Vol. 22, No. 11, doi: 10.1061/(ASCE)BE.1943- 5592.0001125.

Mandić Ivanković, A., Skokandić, D., Žnidarič, A., Kreslin, M. (2017). Bridge performance indicators based on traffic load monitoring. Structure and Infrastructure Engineering, 1–13, doi:10.1080/15732479.2017.1415941.

Melchers, R.E., Beck, A.T. (2018). Structural Reliability Analysis and Prediction, 3rd edition, John Wiley and Sons.

Moura, M.W. (2019). Avaliação Da Confiabilidade de Longarinas de Concreto Protendido de Pontes Rodoviárias em Relação ao Estado Limite Último de Flexão. PhD Thesis, Graduate Program in Civil Engineering, Federal University of Santa Catarina.

Nowak, A.S. (1993). Live load model for highway bridges. Journal of Structural Safety, 13(1#2): 53d66.

Nowak, A.S., Nassif, H., DeFrain, L. (1993). Effect of Truck Loads on Bridges. Journal of Transportation Engineering, 119(6), 853–867, doi:10.1061/(asce)0733-947x(1993)119:6(853).

Nowak, A. S. (1999). Calibration of LRFD Bridge Design Code. Washington, Transportation Research Board.

Nowak, A.S., Szerszen, M.M. (2000). Structural reliability as applied to highway bridges. Progress in Structural Engineering and Materials, 2(2), 218–224, doi:10.1002/1528-2716(200004/06)2:2<218::aid-pse27>3.0.co;2-8.

Nowak, A.S, Collins, K.R. (2012). Reliability of Structures, 2nd edition, CRC Press.

Nowak, A.S., Rakoczy, P. (2013). WIM-based live load for bridges. KSCE Journal of Civil Engineering, 17(3), 568–574, doi:10.1007/s12205-013-0602-8.

O'Brien, E.J., Schmidt, F., Hajializadeh, D., Zhou, X.Y., Enright, B., Caprani, C.C., Wilson, S., and Sheils, E. (2015). A review of probabilistic methods of assessment of load effects in bridges. Structural Safety, Vol. 53, pp. 44-56, doi: 10.1016/j.strusafe.2015. 01.002.

Pais, J. C., Figueiras, H., Pereira, P., & Kaloush, K. (2018). The pavements cost due to traffic overloads. International Journal of Pavement Engineering, 1–11, doi:10.1080/10298436.2018.1435876.

PMC. (2001). Probabilistic Model Code. Joint Committee on Structural Safety, Lyngby.

Portela, E. L., Teixeira, R. M., Bittencourt, T. N., Nassif, H. (2017). Single and multiple presence statistics for bridge live load based on weigh-in-motion data. Revista IBRACON de Estruturas e Materiais, 10(6), 1163–1173, doi:10.1590/s1983-41952017000600002.

Portela, E.L. (2018). Analysis and Development of a Live Load Model for Brazilian Concrete Bridges Based on weight data. Ph.D. Thesis, Polytechnic School of the University of São Paulo.

Ramesh Babu, A., Iatsko, O., Nowak, A.S. (2018). Comparison of Bridge Live Loads in US and Europe. Structural Engineering International, 1-10, doi: 10.1080/10168664. 2018.1541334.

Rossigali, C.E., Pfeil, M. S., Battista, R.C, Sagrilo, L.V. (2015). Towards actual Brazilian traffic load models for short span highway bridges. IBRACON Journal of Structures and Materials, 8(2), 124-139, doi:10.1590/s1983-41952015000200005.

Santiago, W.C., Kroetz, H.M., Santos, S.H.C., Stucchi, F.R., Beck, A.T. (2020). Reliability-based calibration of main Brazilian structural design codes. Latin American Journal of Solids and Structures, v. 17, p. 1-28, 2020, doi: 10.1590/1679-78255754.

Santos, L.F., Pfeil, M.S. (2014). Desenvolvimento de Modelo de Cargas Móveis para Verificação de Fadiga em Pontes Rodoviárias. Engenharia Estudo e Pesquisa, v. 14, p. cap05.

Šavor, Z., Novak, M.Š. (2015). Procedures for reliability assessment of existing bridges. Journal of the Croatian Association of Civil Engineers, 67(6), 557–572, doi: 10.14256/JCE.1190.2014.

Stucchi, F.R., Luchi, L.A.R. e. (2015). Real road load compared to standard load for Brazilian bridges. Proceedings of the Institution of Civil Engineers - Bridge Engineering, 168(3), 245–258, doi:10.1680/jbren.13.00028.

Timerman, J. (2015). Inspeção de pontes: o estágio atual da normalização. São Paulo.

Vitório, J.A.P. (2007). Acidentes estruturais em pontes rodoviárias: Causas, diagnósticos e soluções, II Congresso Brasileiro de Pontes e Estruturas, Rio de Janeiro.

Wang, C., Zhang, H., Li, Q. (2018). Moment-based evaluation of structural reliability. Reliability Engineering & System Safety. doi:10.1016/j.ress.2018.09.006.

APPENDIX A

In this appendix, the CDF referring to the bending moments M_n for each analyzed T and each span are shown. Also, the CDF referring only to the bending moments M_t of the adopted vehicles are presented.
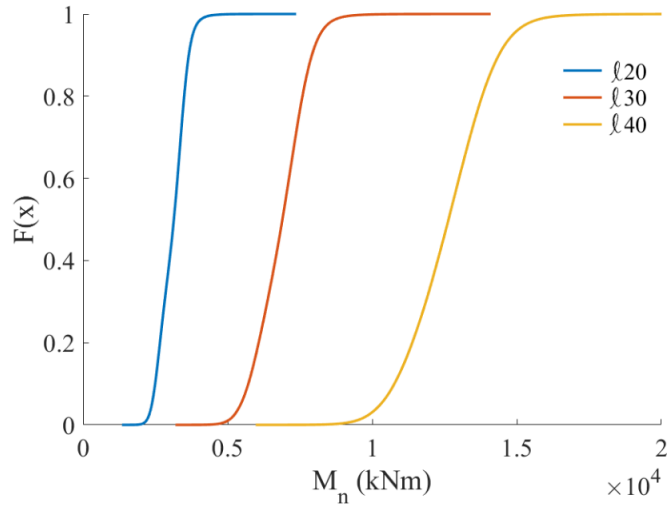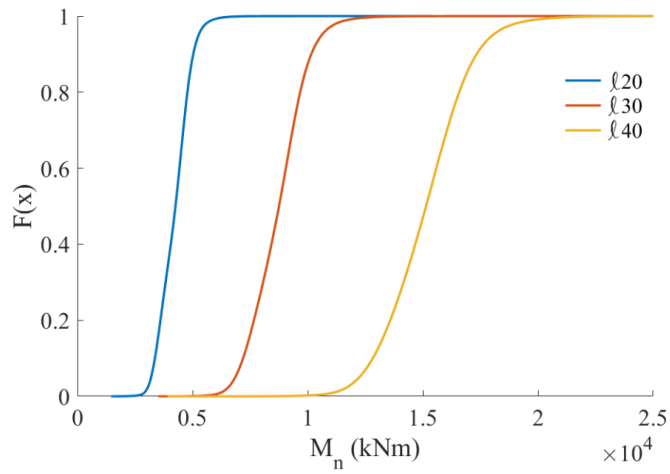

Figure A.1 – CDF for T=0.
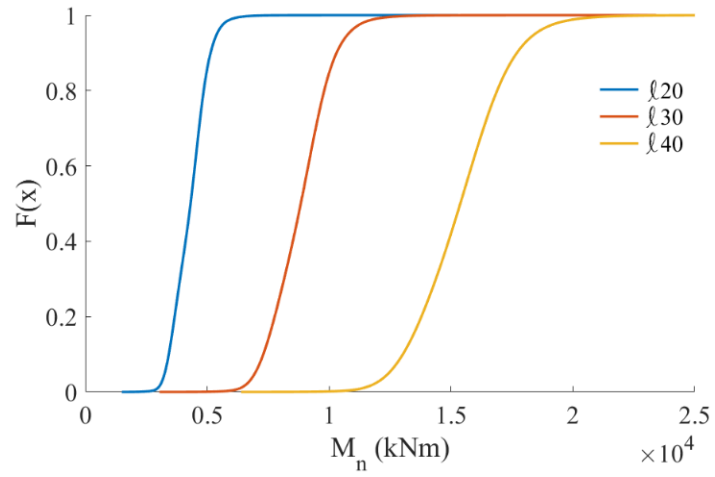

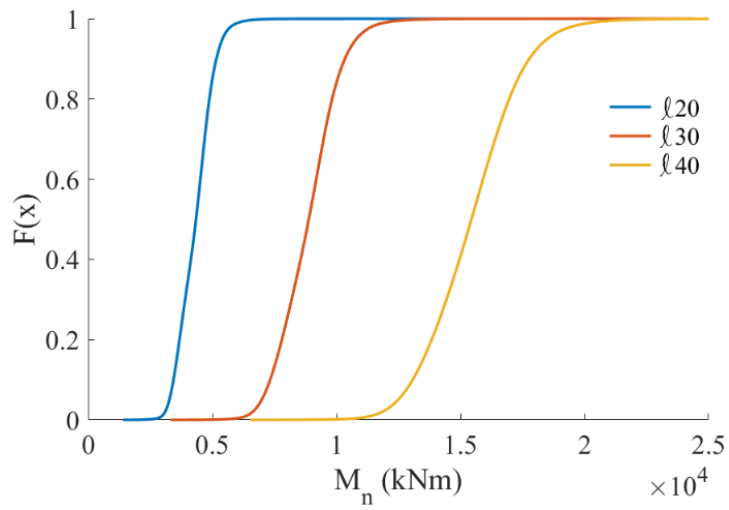Figure A.2 – CDF for T=15.
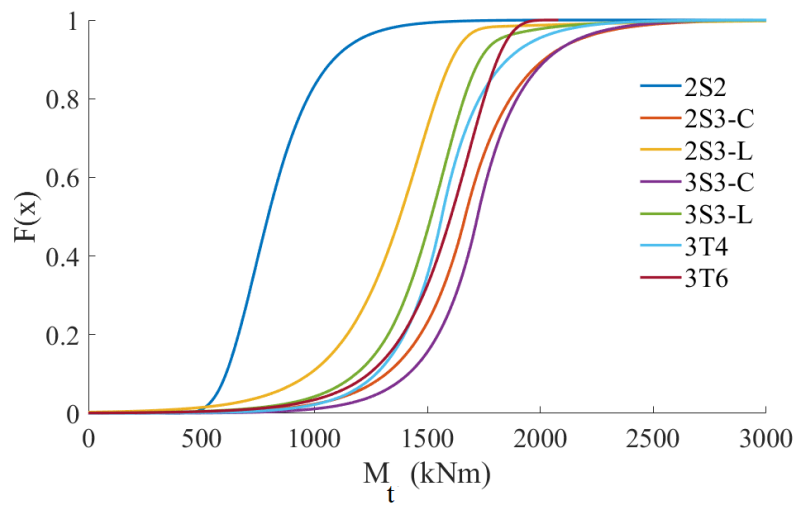
Figure A.3 – CDF for T=50.

Figure A.4 – CDF for T=75.

Figure A.5 – CDF for adopted vehicles in T=0 and ℓ20.
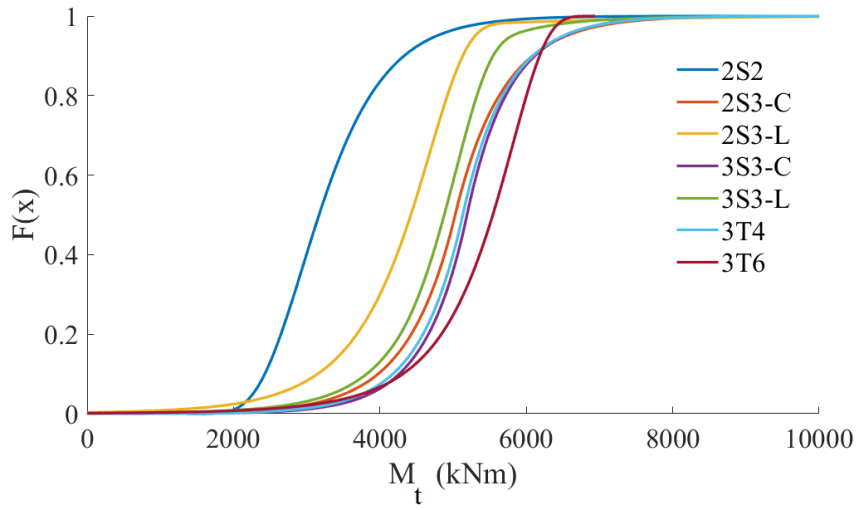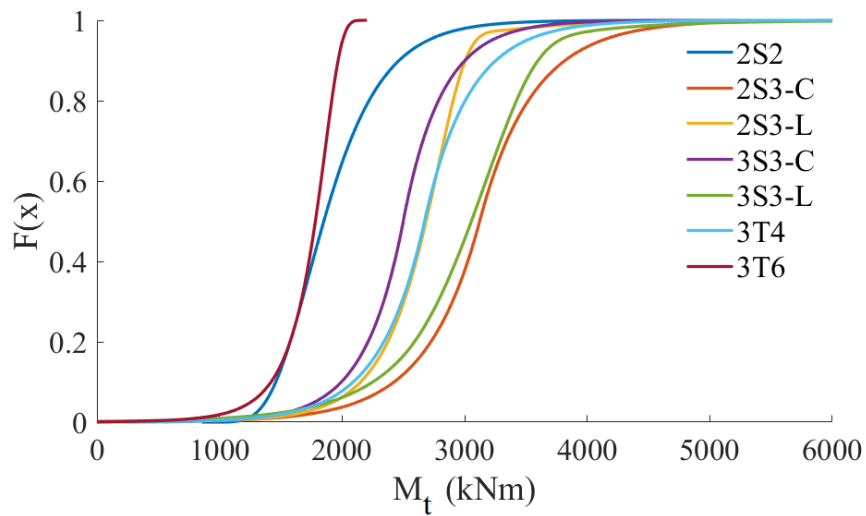
67
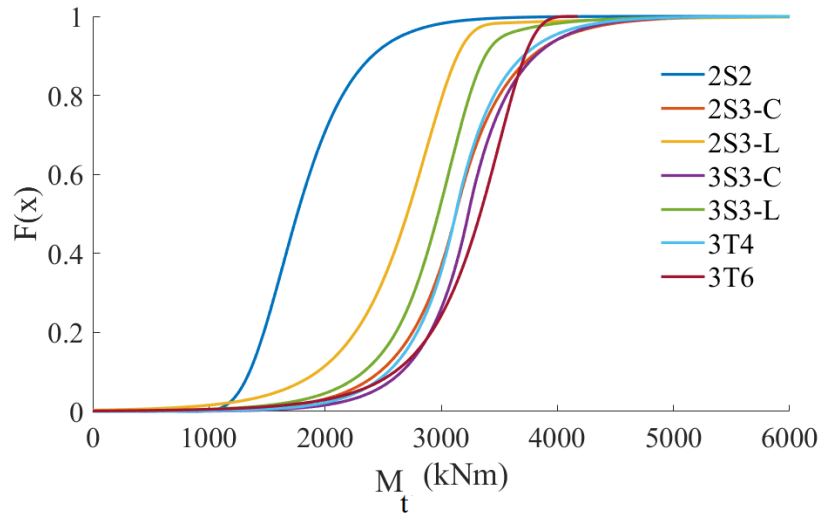
Figure A.6 – CDF for adopted vehicles in T=0 and ℓ30.

Figure A.7 – CDF for adopted vehicles in T=0 and ℓ40.
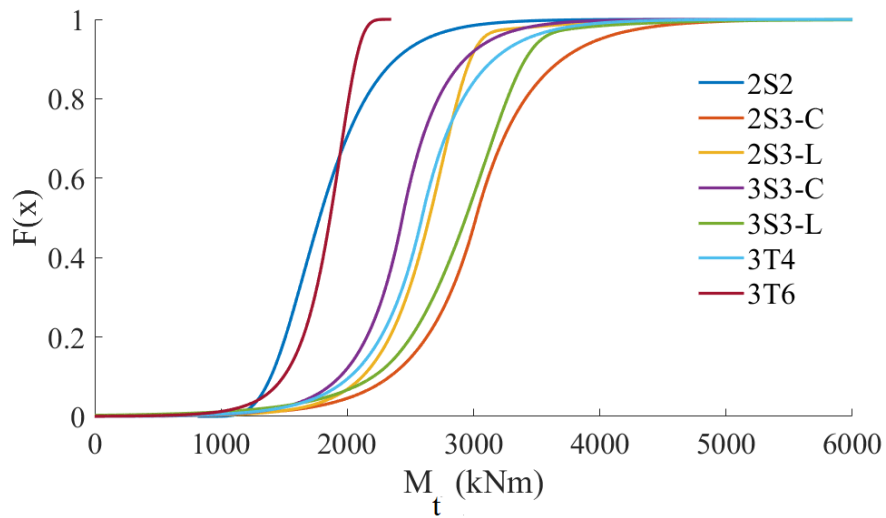
Figure A.8 – CDF for adopted vehicles in T=15 and ℓ20.

68
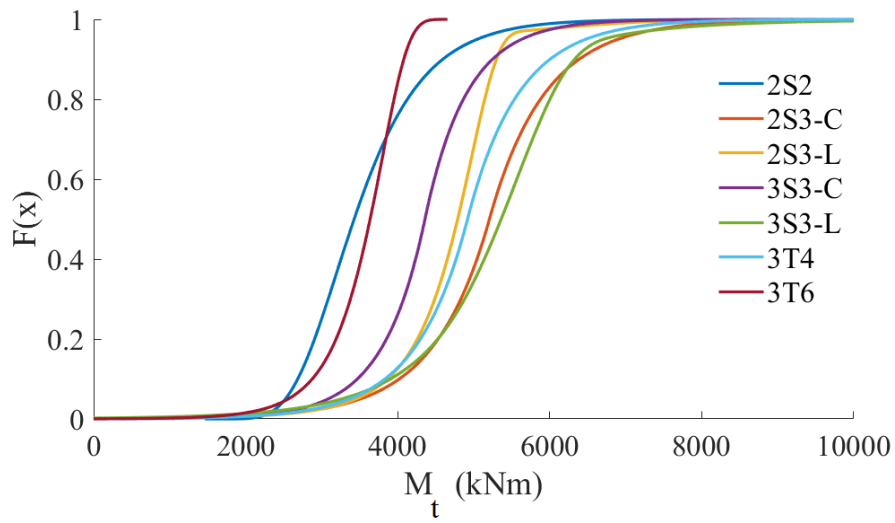
Figure A.9 – CDF for adopted vehicles in T=15 and ℓ30.
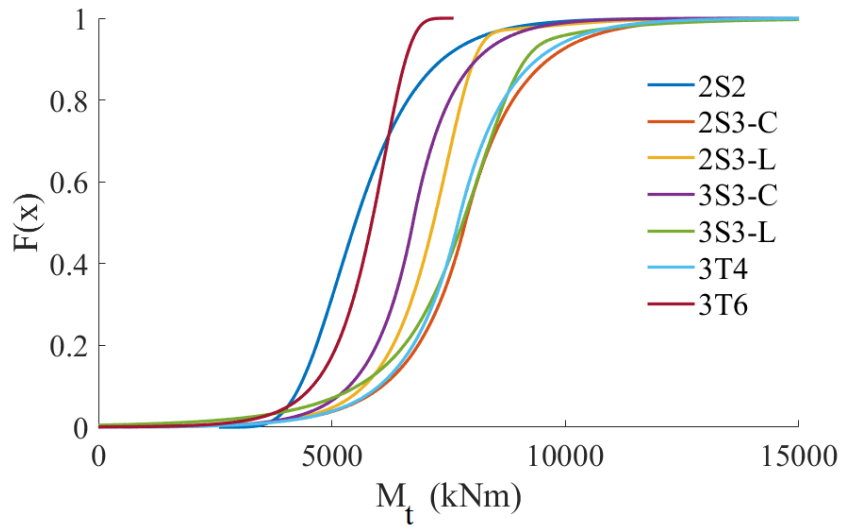
Figure A.10 – CDF for adopted vehicles in T=15 and ℓ40.
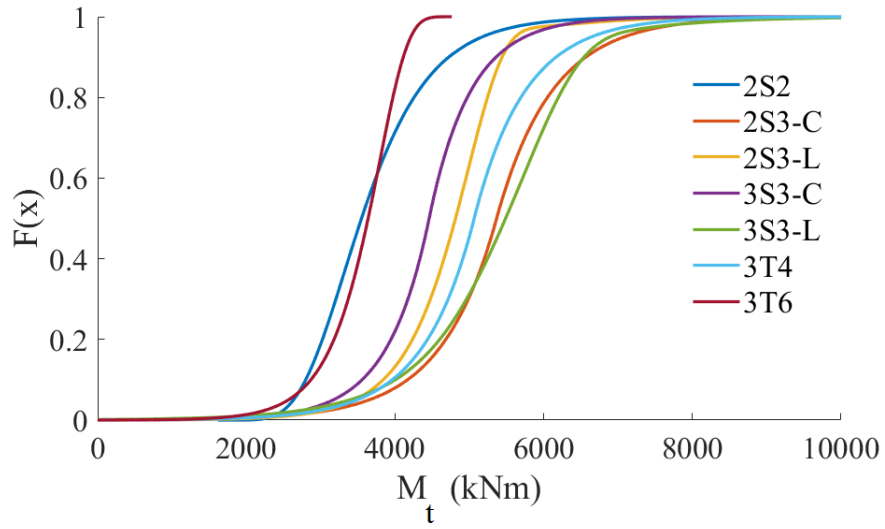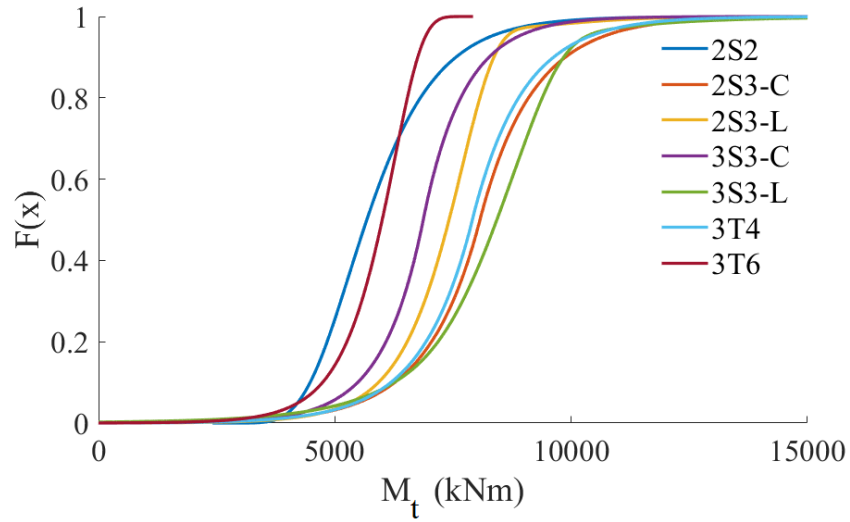

Figure A.11 – CDF for adopted vehicles in T=50 and ℓ20.

Figure A.12 – CDF for adopted vehicles in T=50 and ℓ30.
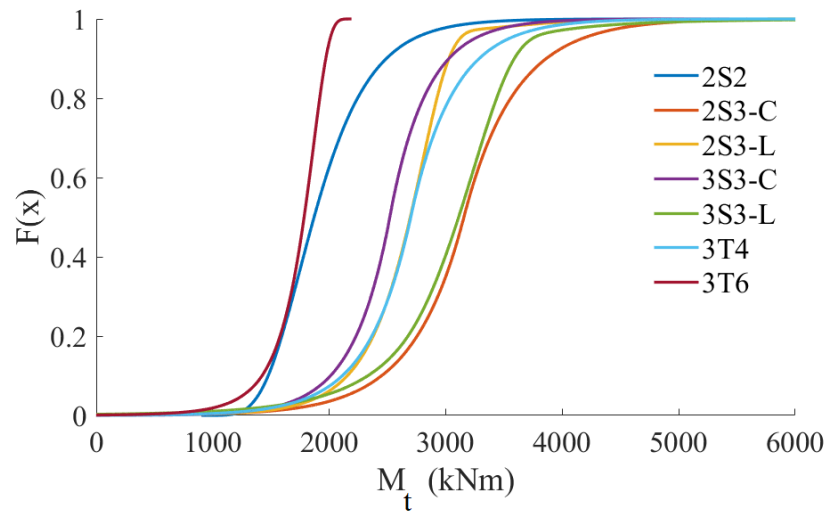

Figure A.13 – CDF for adopted vehicles in T=50 and ℓ40.

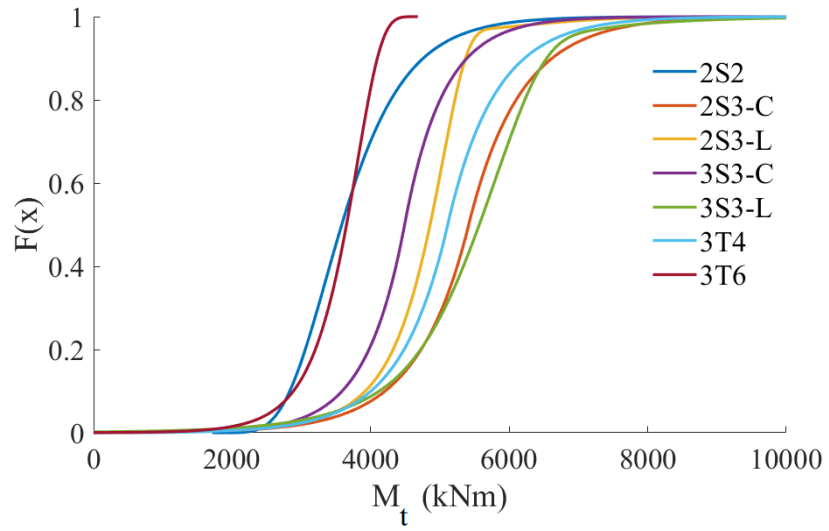
Figure A.14 – CDF for adopted vehicles in T=75 and ℓ20.

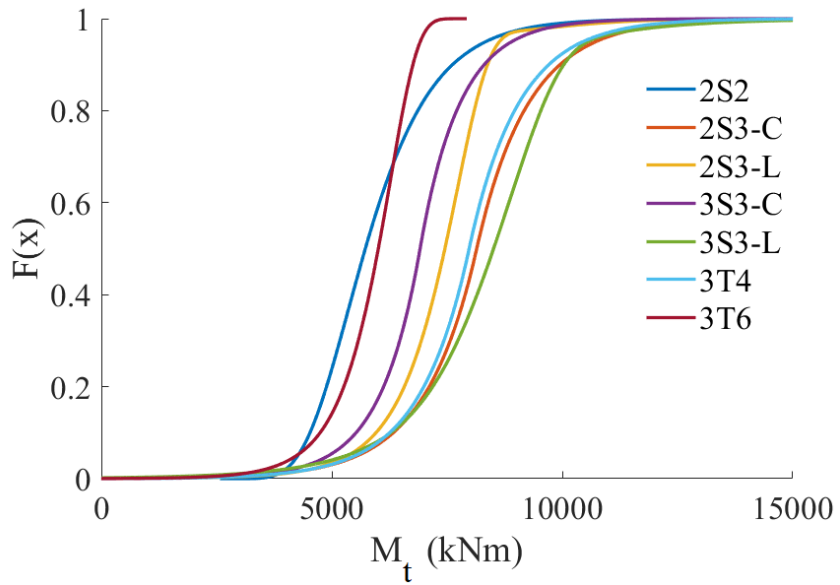Figure A.15 – CDF for adopted vehicles in T=75 and ℓ30.

Figure A.16 – CDF for adopted vehicles in T=75 and ℓ40.